

Homogeneous hydrogenation of saturated bicarbonate slurry to formates using multiphase catalysis

Christophe Rebreyend,^a Evgeny A. Pidko^{a*} and Georgy A. Filonenko^{a*}

[a] Dr. C. Rebreyend, Prof. dr. E. A. Pidko, Dr. G. A. Filonenko
Department of Chemical Engineering
Faculty of Applied Sciences, technical University Delft
van der Maasweg 9, 2629 HZ Delft, the Netherlands.
E-mail: G.A.Filonenko@tudelft.nl, E.A.Pidko@tudelft.nl

Supporting information for this article is given via a link at the end of the document.

Abstract: Formic acid and formate salts are key intermediates along the pathways for CO₂ utilization and hydrogen storage. Herein we report a highly efficient multiphase catalytic system utilizing ruthenium PNP pincer catalyst for converting supersaturated bicarbonate solutions and slurries to aqueous formate solutions up to 12M in molarity. The biphasic catalytic system delivers turnover frequencies up to 73 000 h⁻¹ and remains stable for up to 474'000 turnovers once reaction conditions are optimized.

Among the various CO₂ utilization strategies, its chemical conversion to C₁ building blocks have been the focus of intense research effort over the last decades.^[1] The common utilization routes rely on CO₂ reduction that can be performed electrochemically^[2] or utilize molecular hydrogen as a reducing agent.^[3] The latter can be further split into heterogeneous processes that mainly target methanol as a main product and homogeneous reduction protocols that typically produce formic acid and its salts.^[4] Although recent years have seen significant progress in base metal catalysts for CO₂ hydrogenation, namely iron,^[5] cobalt^[6] and manganese,^[7] the state-of-the-art in homogeneous CO₂ hydrogenation is dominated by noble metal catalysts. Figure 1 depicts several representative examples of such complexes. One of the first highly active CO₂ hydrogenation catalysts reported by Nozaki and co-workers^[4a] (**2**, Figure 1) shows exceptional turnover frequencies (TOFs) up to 150 000 h⁻¹ in hydrogenating CO₂ in the presence of aqueous KOH/THF mixtures at 120-200°C. A family of iridium catalysts reported by Himeda and co-workers^[4a, 4b, 4f, 4g, 8] with complex **3** (Figure 1) as a representative example were also noted for their CO₂ hydrogenation activity pronounced in aqueous at room temperature and 1 bar of hydrogen pressure. Importantly, operation of these complexes could be switched between CO₂ hydrogenation and formic acid dehydrogenation by controlling pH of the reaction solution. Finally, our group reported the highly active ruthenium catalyst (**1**, Figure 1), which was active for both CO₂ hydrogenation and formate dehydrogenation albeit in organic solvents in the presence of organic bases.

From the process standpoint, homogeneous CO₂ hydrogenation should fulfil several requirements to be practical. Firstly, the catalyst should be sufficiently stable to provide high, economically relevant productivity. Secondly, the catalyst should be separable from the formate product that can easily be dehydrogenated once the hydrogenation reactor is decompressed. The latter have recently been addressed by immobilizing homogeneous catalysts on solid supports^[9] and encapsulating them into porous carriers.^[10] While this approach greatly simplifies catalyst separation, it has a drawback of

consistently lower activity of immobilized catalyst compared to its free molecular predecessor.

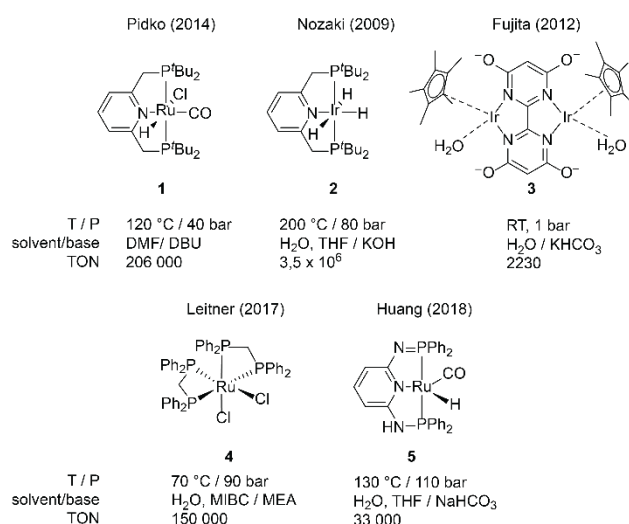


Figure 1. (a) Representative homogeneous catalysts for the hydrogenation of CO₂ to formates and (b) examples of catalysts operating in biphasic systems, allowing for easy product separation.

An approach alternative to immobilization makes use of the biphasic solvent systems,^[11] in which the catalyst and reactants reside in different phases. Formate salts typically reside in aqueous phase while the organometallic catalyst species remain in the organic phase and the catalyst and product(s) separation in biphasic system can be done by simple decantation. Successful utilization of biphasic catalyst system for CO₂ hydrogenation has been demonstrated with catalysts **4**^[11a] and **5**^[11b] shown above and development of highly active biphasic CO₂ hydrogenation is our primary goal in this work.

Herein we report the development of a highly active multiphase catalyst system based on our Ru-PNP catalyst **1** enabling hydrogenation of supersaturated aqueous bicarbonate to formate with outstanding efficiency. While complex **1** is a highly competent catalyst in fully organic media, e.g. DMF/DBU system utilized in earlier studies^[4c] it performed poorly in aqueous environment. Our initial trials using **1** at 40 bar of equimolar H₂/CO₂ in water in the presence of KOH base provided very low formate yields (Table 1, entries 3 and 6) with maximal TON of 1573 at 90 °C. Assuming the low solubility of **1** to be the major factor limiting catalytic performance in the aqueous media, we

performed CO₂ hydrogenation tests in the presence of additional organic solvent. Both a water-miscible DMF and immiscible toluene addition could improve the formate yields (Table 1), however the KOH conversion remained limited to a maximum of 26%. We envisioned that such limitation might stem from the poor transport of ionic species across the phase boundary and employed a phase-transfer catalyst (PTC, methyltriocylammonium chloride) to enhance it. Addition of PTC resulted in a significant increase of formate yields in biphasic catalytic system (Table 2).

Table 1. Solvent effect on the hydrogenation of CO₂ with KOH as the base.^a

Entry	Solvent	KOH (mmol)	TON	Yield (%)
1	H ₂ O/DMF	2.5	5627	26
2	H ₂ O/toluene	2.5	3125	13
3	H ₂ O	2.5	745	3.3
4	H ₂ O/DMF	5.0	7610	18
5	H ₂ O/toluene	5.0	2992	7.5
6	H ₂ O	5.0	1573	3.7

[a] Reaction conditions: 2 mL total solvent (1/1 in case of mixed solvent systems), 0.107 μmol of catalyst **1**, T = 90 °C, p = 40 bar (p_{H₂} = p_{CO₂} = 20 bar), t = 3h.

Table 2. Effect of using methyltriocylammonium chloride as a phase-transfer catalyst in the hydrogenation of CO₂ in biphasic system, using KOH as a base.^a

Entry	PTC (mmol)	KOH (mmol)	TON	Yield (%)
1	no	2.5	3125	13
2	no	5.0	2992	7.5
3	0.025	5.0	20060	52
4	0.29	5.0	17732	46
5	0.052	14	16509	14

[a] Reaction conditions: 2 mL total solvent (H₂O/toluene = 1/1), 0.107 μmol of catalyst **1**, T = 90 °C, p = 40 bar (p_{H₂} = p_{CO₂} = 20 bar), PTC is methyltriocylammonium chloride, t = 3h.

In the same screening experiment we noted that elevated base concentrations consistently resulted in lower formate yields, implying the limited stability of **1** in a highly alkaline medium (Table 2). Circumventing this, we opted to perform direct hydrogenation of bicarbonates – a process with additional advantage of using hydrogen as the only gaseous feedstock. Similar to H₂O/KOH system, the hydrogenation of H₂O/KHCO₃ shows a limited efficiency in pure water or in the absence of a PTC (Table 3). However, a biphasic medium with PTC provides excellent TON values > 100 000 with yields significantly higher than those found with potassium hydroxide base (Table 3).

Table 3. Hydrogenation of potassium bicarbonate, with and without using a phase-transfer catalyst.^a

Entry	Solvent	PTC (mmol)	KHCO ₃ (mmol)	TON	Yield (%)
1	H ₂ O	No	10	3963	4.5
2	H ₂ O/toluene	No	10	4263	4.8
3	H ₂ O/toluene	0.055	10	66495	78
4	toluene	0.055	5.0	289	0.6
5	H ₂ O/toluene	0.055	5.0	26897	65
6	H ₂ O/toluene	0.055	14	102593	86

^a Reaction conditions: 2 mL total solvent (1/1 in case of mixed solvent systems), 0.107 μmol of catalyst **1**, T = 90 °C, p = 40 bar (p_{H₂} = 40 bar), t = 3h, PTC = methyltriocylammonium chloride.

In sharp contrast with hydroxide bases, a gradual increase of KHCO₃ loading leads to the marked increase in both observed TON and final formate yield. For example, we could utilize KHCO₃ loadings of up to 14 mmol/mL_{H₂O} and obtain final yields in extent of 86 % corresponding to TON of 102593 (Table 3, entry 6). Remarkably, even at the temperature of 90 °C, reaction mixture is saturated in potassium bicarbonate with the main fraction of KHCO₃ remaining solid. In line with solubility of potassium formate being significantly higher than that of bicarbonate our approach effectively transforms bicarbonate slurries to >50%_{wt} formate solutions with no need for product concentration.

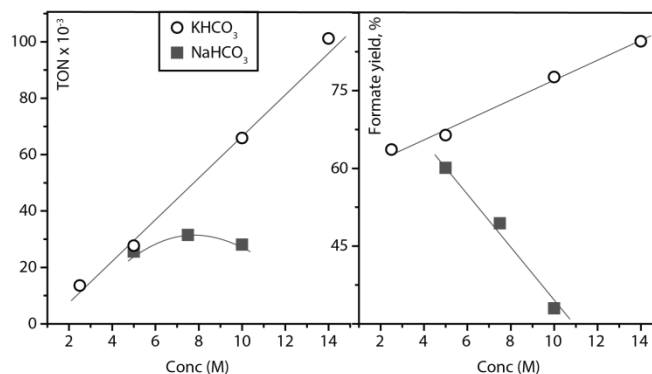


Figure 2. Concentration effects of KHCO₃ and NaHCO₃ on the formate yield and TONs. Reaction conditions: 2 mL solvent total (H₂O/toluene = 1/1), 0.107 μmol of catalyst **1**, 0.055 mmol methyltriocylammonium chloride, T = 90 °C, p = 40 bar (p_{H₂} = 40 bar), t = 4.5 h, concentrations are considered as M/H₂O.

The trend of increasing formate yield as a function of initial bicarbonate loading was confirmed in a separate study depicted in Figure 2. Upon increase of KHCO₃ loading from 2 to 14 mol per litre water, the formate yield increased from 63 to 86 %. Interestingly, catalytic reaction apparently accelerated upon addition of bicarbonate as the registered TON values for hydrogenation also increased from 13 373 to 102 593. Contrary to the case of potassium bicarbonate, NaHCO₃ does not impact catalysis favourably upon the loading increase. Sodium formate yields decrease and TON values calculated as the number of turnovers per that of catalyst molecules remains similar. Considering that identical catalyst loadings were used for all

experiments depicted in Figure 2, our data implies that selection of alkali cation is crucial for producing efficient catalytic system.

Finally, we examined the impact of reaction conditions on the performance of biphasic catalytic system. Varying the reaction temperature and pressure over in series of experiments (Figure 3 and ESI) we confirmed that biphasic hydrogenation exhibits behavior similar to that of single solvent systems. Namely, the increase of reaction temperature from 65 to 120 °C leads to the marked drop in formate yield, while the increase of H₂ pressure from 5 to 60 bar H₂ results in the increased formate yield. This is consistent with expected thermodynamic behavior of the system as well as recent reports detailing this reaction.^[12]

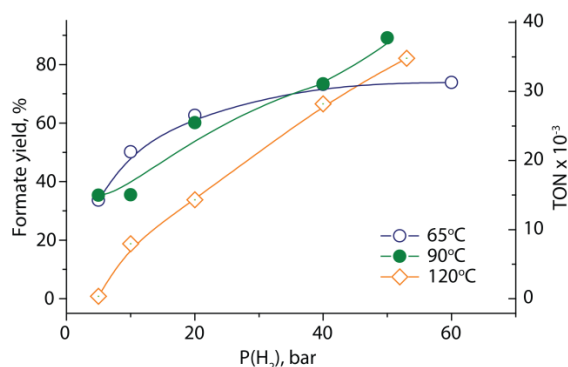


Figure 3. Effect of temperature and pressure on the formate yield and TONs in the hydrogenation of KHCO₃. Reaction conditions: 2 mL solvent, 0.107 μmol of catalyst **1**, 55mM methyltrioctylammonium chloride, t = 16h, KHCO₃ = 5 mmol, T and p are varied.

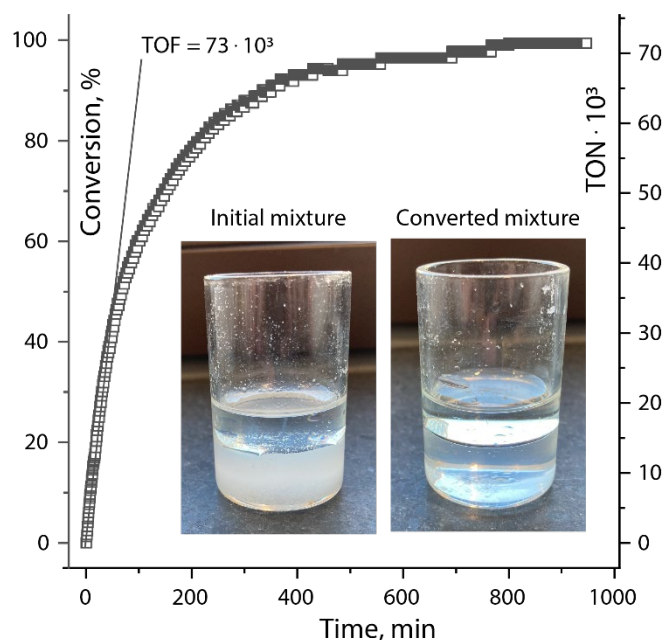


Figure 4. Conversion versus time in the hydrogenation of KHCO₃. Reaction conditions: 10 mL solvent (H₂O/ toluene = 1/1), 0.535 μmol of catalyst **1**, methyltrioctylammonium chloride, T = 90 °C, p = 50 bar (p_{H₂}=50 bar), KHCO₃ = 50 mmol (10M in H₂O). Inside the graph are the stirred reaction mixtures before (left) and after (right) reaction, showing the net conversion of the bicarbonate suspension into a clear solution at RT.

Examining kinetics of bicarbonate hydrogenation we found that **1** is capable of developing high turnover frequencies (TOF) with no apparent inhibition often observed in organic media.^[13] Tracking hydrogen consumption in the course of hydrogenation we estimated initial TOF in extent of 73 000 h⁻¹ (Figure 4) with kinetic traces following a regular monoexponential trendline. These experiments could also confirm the ease of scaling this reaction that was performed on 50 mmol scale as compared to a five-fold lower scale used in screening.

Finally, we probed the performance limits of biphasic catalytic system based on **1**. In order to maximize TON per batch we varied the catalyst concentration and found no significant productivity drop with catalyst concentration as low as 2 ppm with respect to bicarbonate substrate (Table 4). Under these conditions, TON values up to 300 000 can be achieved with similar formate yields in extent of 70 %, producing clear formate solutions at the end of the catalytic reaction.

Table 4. Effect of the concentration of catalyst on the final yield and TON.^a

Entry	Cat (μmol)	TON	Yield (%)
1	0.006	474 026	55
2	0.012	296 756	70
3	0.029	109 224	64
4	0.059	56 996	67
5	0.12	27 728	67

[a] Reaction conditions: 2 mL solvent, 5 mmol KHCO₃, T = 90 °C, p_{H₂} = 40 bar, 0.055 mmol methyltrioctylammonium chloride, t = 18h.

To conclude, in this work we developed a potent catalytic system based on ruthenium complex **1**. Making use of its biphasic composition, our system is capable of converting supersaturated bicarbonate slurries to formate solutions close to their saturation point. We demonstrate generation of ca. 50%_wt aqueous formate solutions from commercial potassium bicarbonate with no substrate purification required prior to catalysis. With a maximum TON of 474 x 10³ catalyst **1** appears very promising for developing intense hydrogenation processes in aqueous medium free of the limitations associated with conventional organic solvents.

Acknowledgements

This research was carried out with the financial support from Nitto Denko Corporation.

Keywords: bicarbonate • catalysis • hydrogenation • formate • multiphasic

- [1] a) P. G. Jessop, T. Ikariya, R. Noyori, *Nature* **1994**, *368*, 231-233; b) Q. Liu, L. Wu, R. Jackstell, M. Beller, *Nat. Commun.* **2015**, *6*, 5933.
- [2] aM.-Y. Lee, K. T. Park, W. Lee, H. Lim, Y. Kwon, S. Kang, *Critical Rev. Environ. Sci. Tech.* **2020**, *50*, 769-815; b) D. H. Apaydin, S. Schlager, E. Portenkirchner, N. S. Sariciftci, *ChemPhysChem* **2017**, *18*, 3094-3116.
- [3] Y. Himeda, *CO₂ Hydrogenation Catalysis*, V. C. H. Wiley, **2021**.

- [4] a) J. F. Hull, Y. Himeda, W.-H. Wang, B. Hashiguchi, R. Periana, D. J. Szalda, J. T. Muckerman, E. Fujita, *Na. Chem.* **2012**, *4*, 383-388; b) N. Onishi, S. Xu, Y. Manaka, Y. Suna, W.-H. Wang, J. T. Muckerman, E. Fujita, Y. Himeda, *Inorg. Chem.* **2015**, *54*, 5114-5123; c) G. A. Filonenko, R. van Putten, E. N. Schulp, E. J. M. Hensen, E. A. Pidko, *ChemCatChem* **2014**, *6*, 1526-1530; d) E. Graf, W. Leitner, *J. Chem. Soc. Chem. Comm.* **1992**, 623-624; e) H. Hayashi, S. Ogo, S. Fukuzumi, *Chem. Commun.* **2004**, 2714-2715; f) Y. Himeda, N. Onozawa-Komatsuzaki, H. Sugihara, H. Arakawa, K. Kasuga, *Organometallics* **2004**, *23*, 1480-1483; g) Y. Himeda, N. Onozawa-Komatsuzaki, H. Sugihara, K. Kasuga, *Organometallics* **2007**, *26*, 702-712; h) C. A. Huff, M. S. Sanford, *ACS Catal.* **2013**, *3*, 2412-2416; i) D. Jantke, L. Pardatscher, M. Drees, M. Cokoja, W. A. Herrmann, F. E. Kühn, *ChemSusChem* **2016**, *9*, 2849-2854; j) P. G. Jessop, Y. Hsiao, T. Ikariya, R. Noyori, *J. Am. Chem. Soc.* **1996**, *118*, 344-355; k) F. Joó, F. Joó, L. Nádásdi, J. Elek, G. Laurenczy, L. Nádásdi, *Chem. Commun.* **1999**, 971-972; l) J. Kothandaraman, M. Czaun, A. Goepfert, R. Haiges, J.-P. Jones, R. B. May, G. K. S. Prakash, G. A. Olah, *ChemSusChem* **2015**, *8*, 1442-1451; m) S.-M. Lu, Z. Wang, J. Li, J. Xiao, C. Li, *Green Chem.* **2016**, *18*, 4553-4558; n) Y. Maenaka, T. Suenobu, S. Fukuzumi, *Energy Environ. Sc.* **2012**, *5*, 7360-7367; o) S. Oldenhof, J. I. van der Vlugt, J. N. H. Reek, *Catal. Sci. Technol.* **2016**, *6*, 404-408; p) T. J. Schmeier, G. E. Dobreiner, R. H. Crabtree, N. Hazari, *J. Am. Chem. Soc.* **2011**, *133*, 9274-9277; q) R. Tanaka, M. Yamashita, K. Nozaki, *J. Am. Chem. Soc.* **2009**, *131*, 14168-14169.
- [5] a) C. Federsel, A. Boddien, R. Jackstell, R. Jennerjahn, P. J. Dyson, R. Scopelliti, G. Laurenczy, M. Beller, *Angew. Chem. Int. Ed.* **2010**, *49*, 9777-9780; b) R. Langer, Y. Diskin-Posner, G. Leitner, L. J. W. Shimon, Y. Ben-David, D. Milstein, *Angew. Chem. Int. Ed.* **2011**, *50*, 9948-9952; c) Y. Zhang, A. D. MacIntosh, J. L. Wong, E. A. Bielinski, P. G. Williard, B. Q. Mercado, N. Hazari, W. H. Bernskoetter, *Chem. Sci.* **2015**, *6*, 4291-4299; d) C. Ziebart, C. Federsel, P. Anbarasan, R. Jackstell, W. Baumann, A. Spannenberg, M. Beller, *J. Am. Chem. Soc.* **2012**, *134*, 20701-20704; e) F. Bertini, N. Gorgas, B. Stöger, M. Peruzzini, L. F. Veiros, K. Kirchner, L. Gonsalvi, *ACS Catal.* **2016**, *6*, 2889-2893.
- [6] a) J. Choi, Y. Lee, *Inorg. Chem. Frontiers* **2020**, *7*, 1845-1850; b) C. Federsel, C. Ziebart, R. Jackstell, W. Baumann, M. Beller, *Chem. Eur. J.* **2012**, *18*, 72-75; c) M. S. Jeletic, M. T. Mock, A. M. Appel, J. C. Linehan, *J. Am. Chem. Soc.* **2013**, *135*, 11533-11536; d) J. Schneidewind, R. Adam, W. Baumann, R. Jackstell, M. Beller, *Angew. Chem. Int. Ed.* **2017**, *56*, 1890-1893.
- [7] a) F. Bertini, M. Glatz, N. Gorgas, B. Stöger, M. Peruzzini, L. F. Veiros, K. Kirchner, L. Gonsalvi, *Chem. Sci.* **2017**, *8*, 5024-5029; b) A. Dubey, L. Nencini, R. R. Fayzullin, C. Nervi, J. R. Khusnutdinova, *ACS Catal.* **2017**, *7*, 3864-3868; c) S. Kar, A. Goepfert, J. Kothandaraman, G. K. S. Prakash, *ACS Catal.* **2017**, *7*, 6347-6351.
- [8] a) R. Kanega, M. Z. Ertem, N. Onishi, D. J. Szalda, E. Fujita, Y. Himeda, *Organometallics* **2020**, *39*, 1519-1531; b) S. Xu, N. Onishi, A. Tsurusaki, Y. Manaka, W.-H. Wang, J. T. Muckerman, E. Fujita, Y. Himeda, *Eur. J. Inorg. Chem.* **2015**, 5591-5594.
- [9] B. Chen, M. Dong, S. Liu, Z. Xie, J. Yang, S. Li, Y. Wang, J. Du, H. Liu, B. Han, *ACS Catal.* **2020**, *10*, 8557-8566.
- [10] a) Z. Li, T. M. Rayder, L. Luo, J. A. Byers, C.-K. Tsung, *J. Am. Chem. Soc.* **2018**, *140*, 8082-8085; b) C. Wu, F. Irshad, M. Luo, Y. Zhao, X. Ma, S. Wang, *ChemCatChem* **2019**, *11*, 1256-1263.
- [11] a) M. Scott, B. Blas Molinos, C. Westhues, G. Franciò, W. Leitner, *ChemSusChem* **2017**, *10*, 1085-1093; b) C. Guan, Y. Pan, E. P. L. Ang, J. Hu, C. Yao, M.-H. Huang, H. Li, Z. Lai, K.-W. Huang, *Green Chem.* **2018**, *20*, 4201-4205.
- [12] A. Weiland, S. P. Argent, V. Sans, *Nat. Commun.* **2021**, *12*, 231.
- [13] G. A. Filonenko, M. P. Conley, C. Copéret, M. Lutz, E. J. M. Hensen, E. A. Pidko, *ACS Catal.* **2013**, *3*, 2522-2526.



SUPPORTING INFORMATION

Homogeneous hydrogenation of saturated bicarbonate slurry to formates using multiphase catalysis

Christophe Rebreyend,^a Evgeny A. Pidko^{a*} and Georgy A. Filonenko^{a*}

[a] Inorganic Systems Engineering group, Department of Chemical Engineering, Delft University of Technology, The Netherlands

Corresponding authors: Evgeny A. Pidko (e.a.pidko@tudelft.nl)

Georgy A. Filonenko (g.a.filonenko@tudelft.nl)

S1. General considerations

All manipulations were, unless stated otherwise, performed under inert atmosphere in an argon filled glovebox (INERT) or using standard Schlenk techniques. Anhydrous solvents were either dispensed from an Inert PureSolv solvent purification system or dried using 3/4 Å molecular sieves and were degassed before use. Chemicals were purchased from Sigma-Aldrich, Strem, abcr or TCI. Air and/or moisture sensitive materials were stored in the glovebox. Deuterated solvents were purchased from Eurisotop, dried using molecular sieves, degassed and stored in the glovebox.

NMR spectra were recorded on an Agilent 400-MR DD2 400 MHz spectrometer equipped with a 5 mm ONE NMR probe. All ^{13}C and ^{31}P NMR spectra were recorded with ^1H decoupling. All chemical shifts were referenced to residual solvent peaks [D_2O : 4.79 ppm (^1H), CDCl_3 : 7.26 ppm (^1H), 77.2 ppm (^{13}C)].

Complex **1** was prepared according to a literature procedure.¹

S2. General considerations

General procedure for catalytic hydrogenation of CO_2 in presence of KOH

Stock solutions of **1** (0.012 M) were prepared in dimethylformamide solvent. In a typical run, potassium hydroxide, methyltrioctylammonium chloride (24 mg, 55 μmol), toluene (1 mL), water (1 mL) and appropriate amount of the stock solution of complex **1** were combined in this order in a 4 mL glass vial equipped with a rare-earth stirring bar and transferred into a stainless steel autoclave in the glovebox. The system was purged with argon (5×8 bar) and H_2 (7×10 bar), pressurized with H_2 to 3 bar, and heated to specified temperature, after which the H_2 and CO_2 were regulated to the desired pressure. After the desired reaction time, the autoclave was cooled and the pressure released, after which DMSO was added as an internal standard (100 μL , 1.408 mmol). A 100 μL aliquot of the H_2O layer was dissolved in D_2O and the yield determined by ^1H NMR analysis.

General procedure for catalytic hydrogenation of potassium bicarbonate

Stock solutions of **1** (0.012 M) were prepared in dimethylformamide solvent. In a typical run, potassium bicarbonate, methyltrioctylammonium chloride (24 mg, 55 μmol), toluene (1 mL), water (1 mL) and appropriate amount of the stock solution of complex **1** were combined in this order in a 4 mL glass vial equipped with a rare-earth stirring bar and transferred into a stainless steel autoclave in the glovebox. The system was purged with argon (5×8 bar) and H_2 (7×10 bar), pressurized with H_2 to 5 bar, and heated to specified temperature, after which the H_2 was regulated to the desired pressure. After the desired reaction time, the autoclave was cooled and the pressure released, after which DMSO

was added as an internal standard (100 μL , 1.408 mmol). A 100 μL aliquot of the H_2O layer was dissolved in D_2O and the yield determined by ^1H NMR analysis.

¹H NMR data accompanying data provided in Table 1

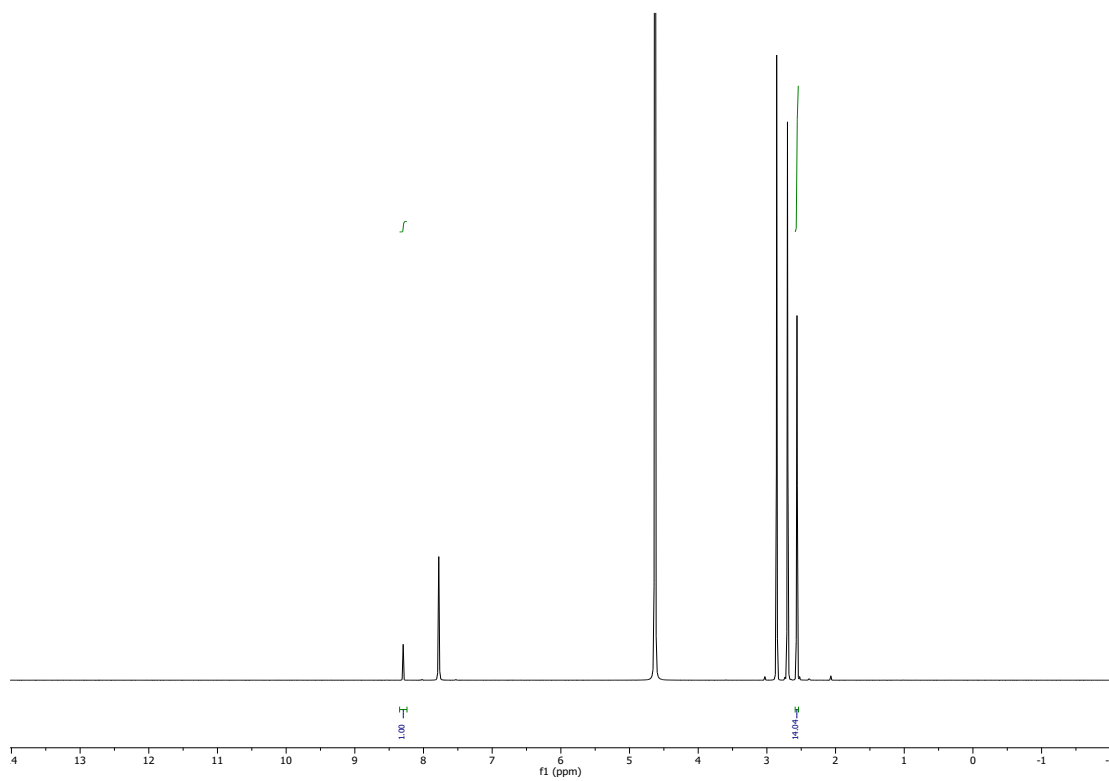


Figure S1. NMR data belonging to table 1, entry 1.

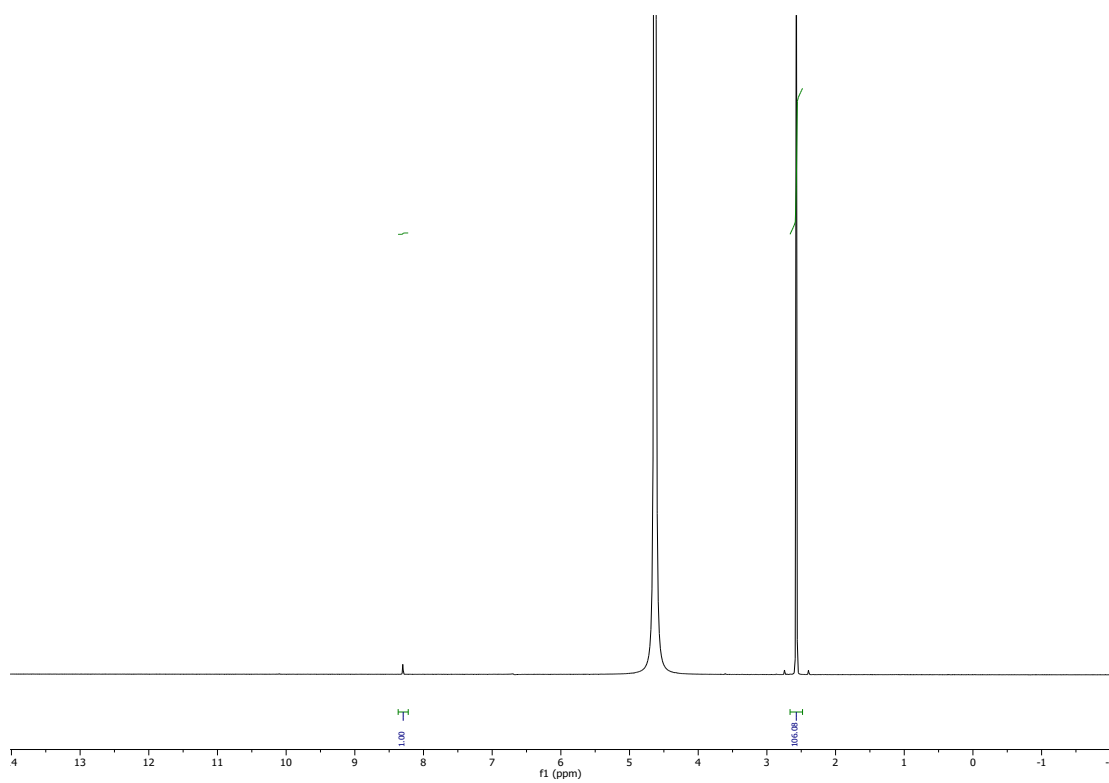


Figure S2. NMR data belonging to table 1, entry 2.

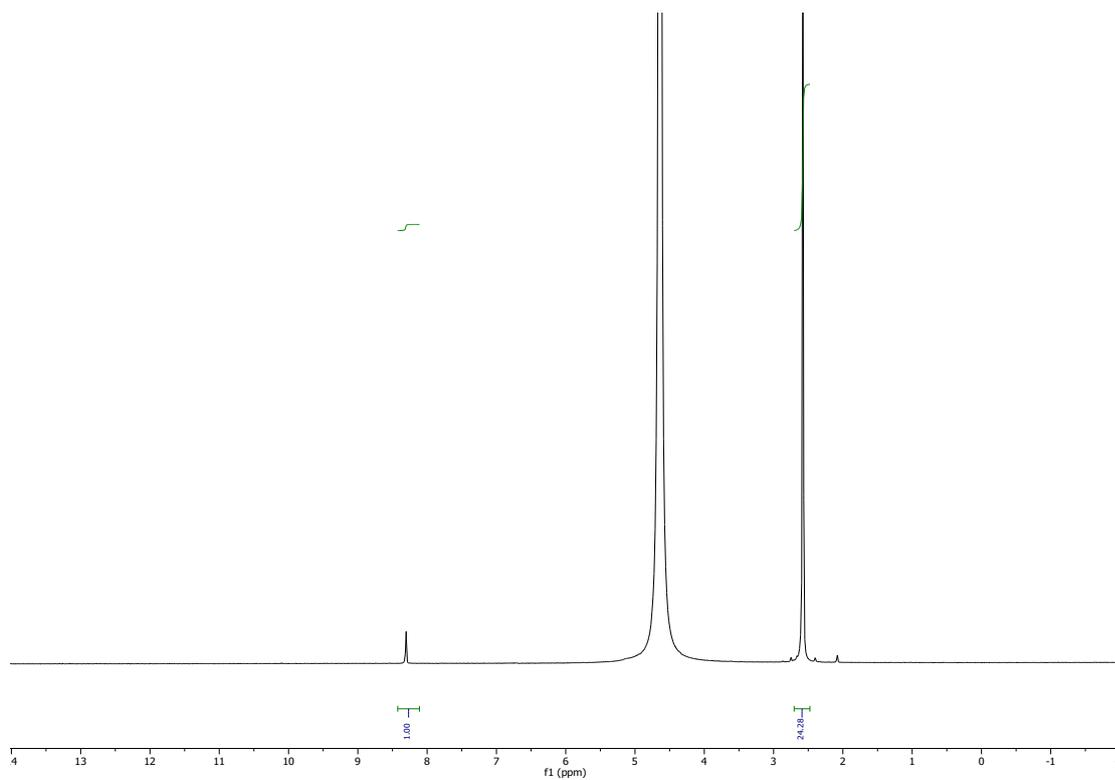


Figure S3. NMR data belonging to table 1, entry 3.

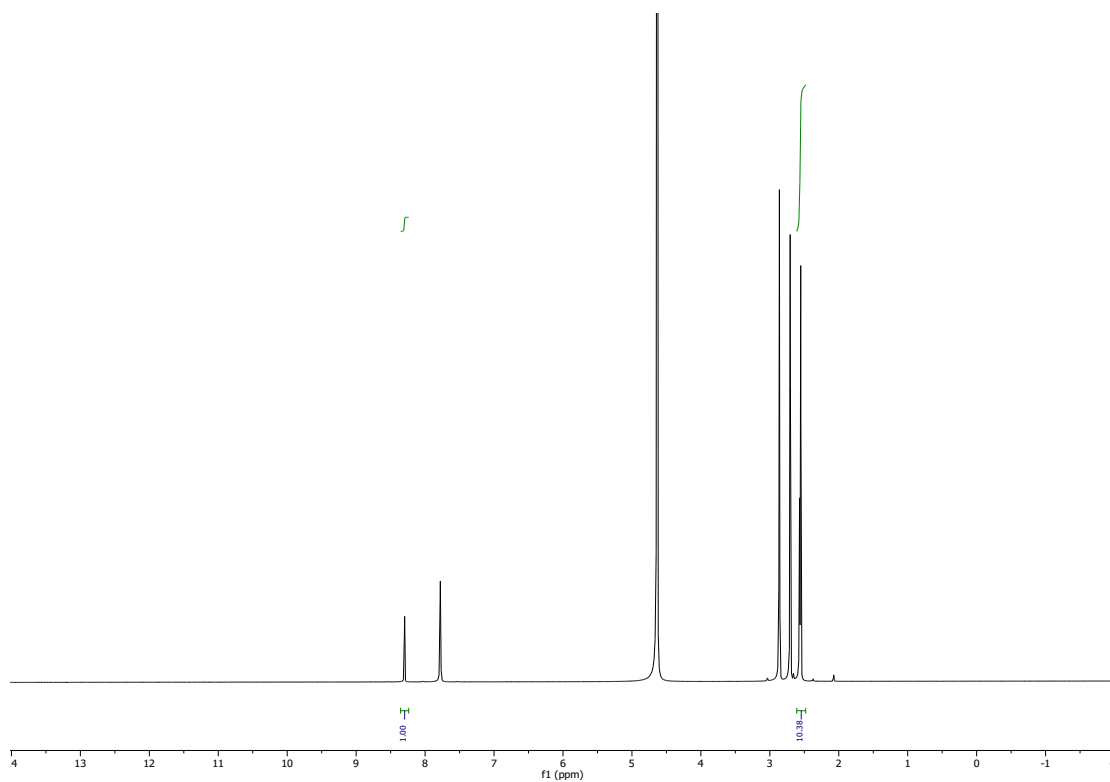


Figure S4. NMR data belonging to table 1, entry 4.

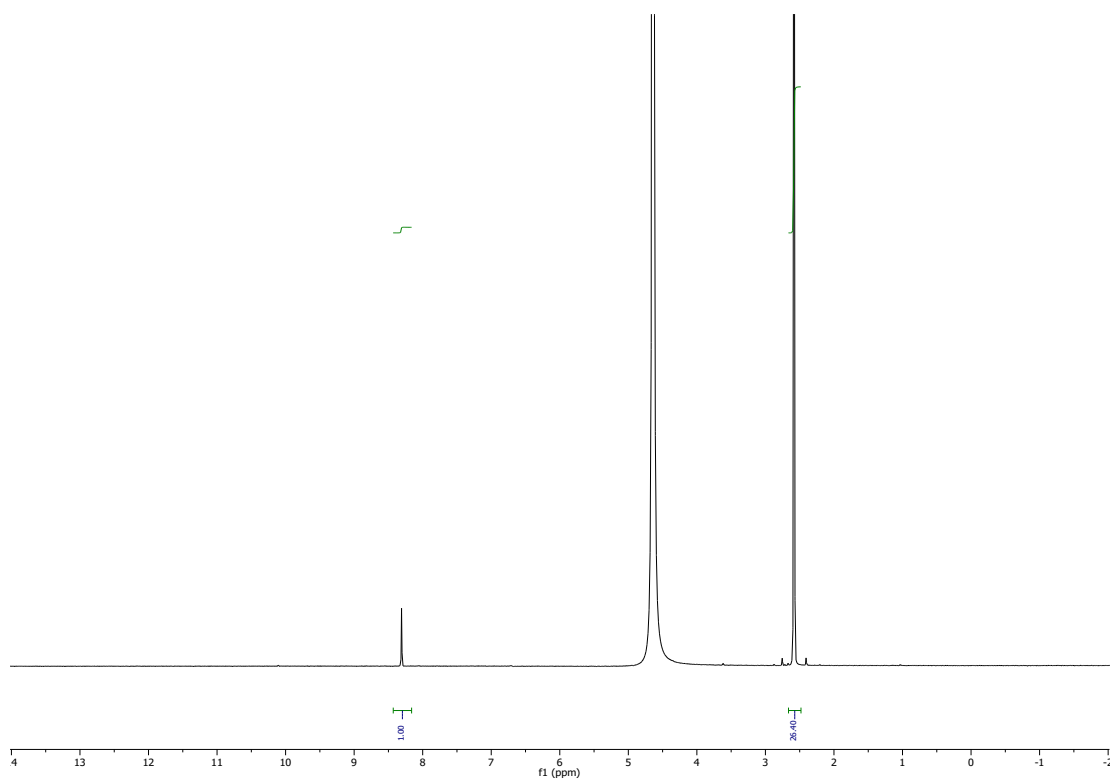


Figure S5. NMR data belonging to table 1, entry 5.

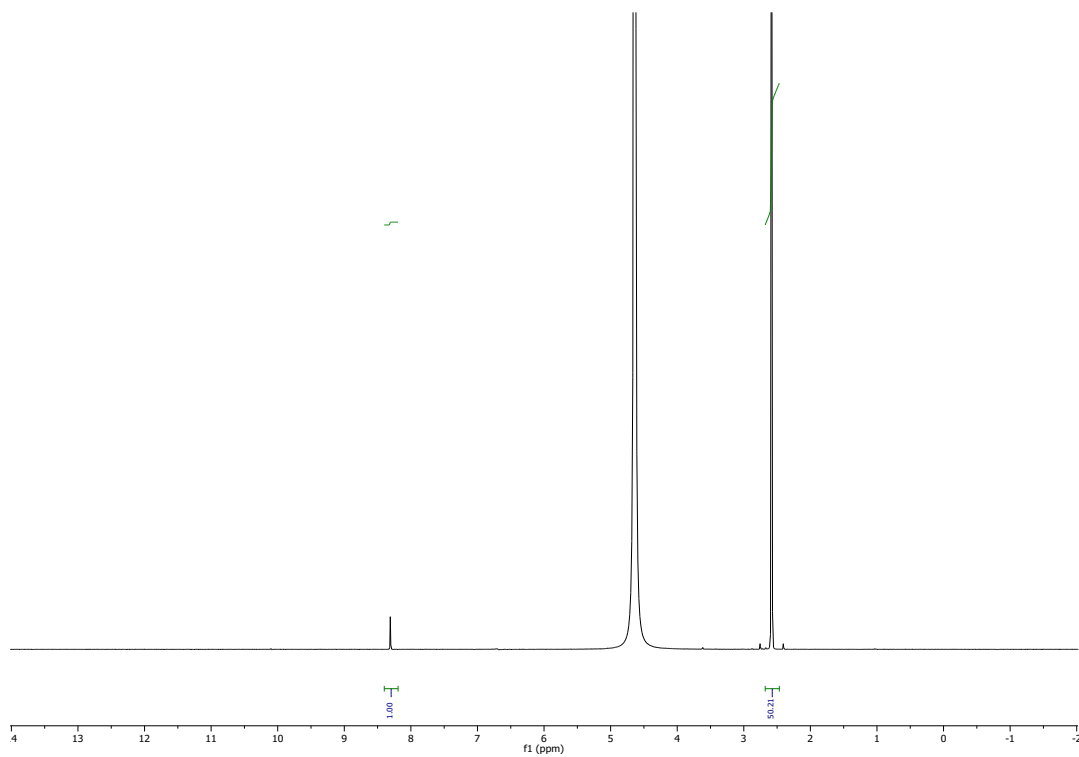


Figure S6. NMR data belonging to table 1, entry 6.

Table S1. ^1H NMR peak data belonging to table 1 (main text) and Figures S1-S6.

Entry	Ratio of DMSO to formate integral
1	14.04
2	24.28
3	106.08
4	10.38
5	26.40
6	50.21

¹H NMR data accompanying data provided in Table 2

NB: Entries 1-2 are covered in Figure S3 and Figure S6.

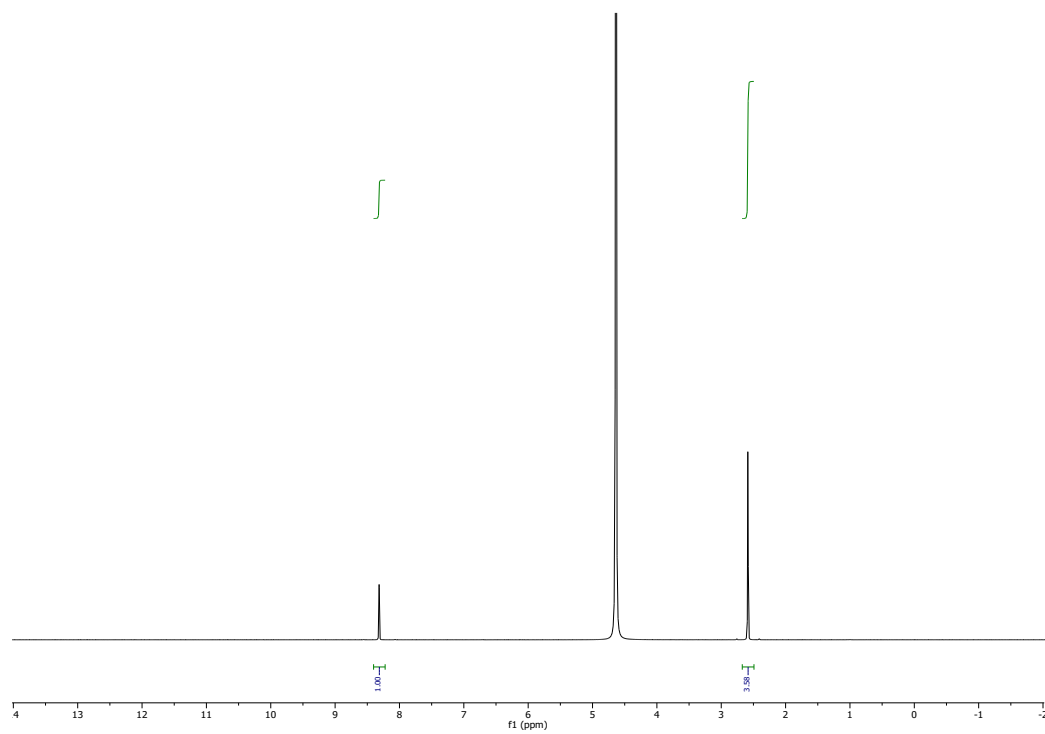


Figure S7. NMR data belonging to table 2, entry 3.

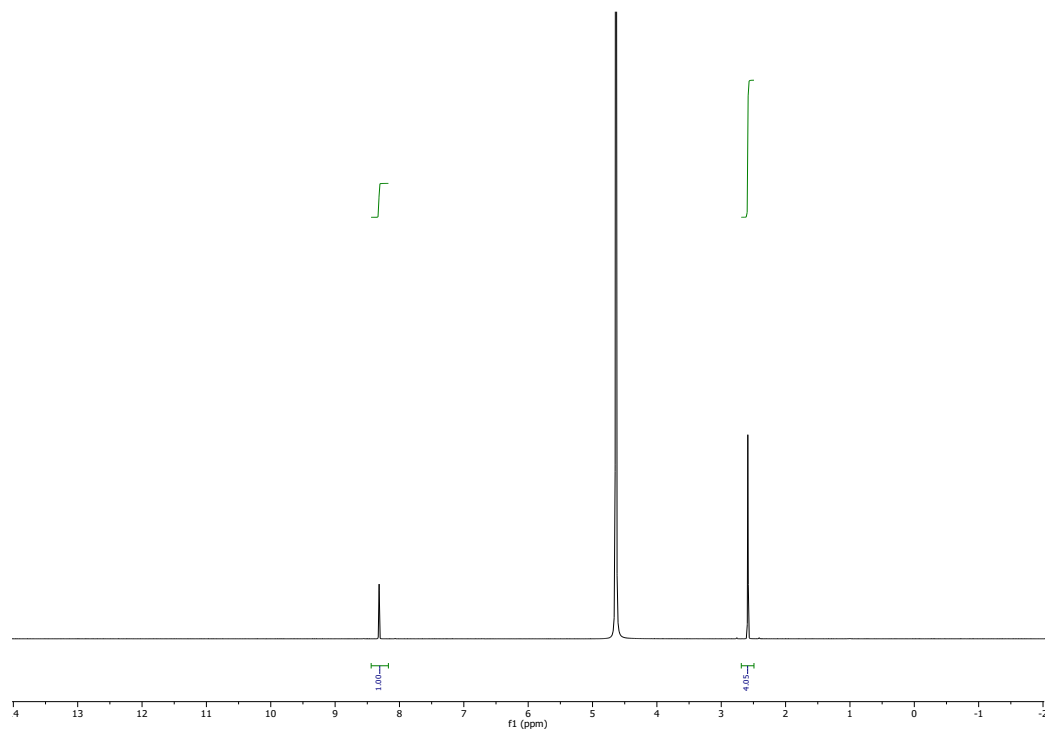


Figure S8. NMR data belonging to table 2, entry 4.

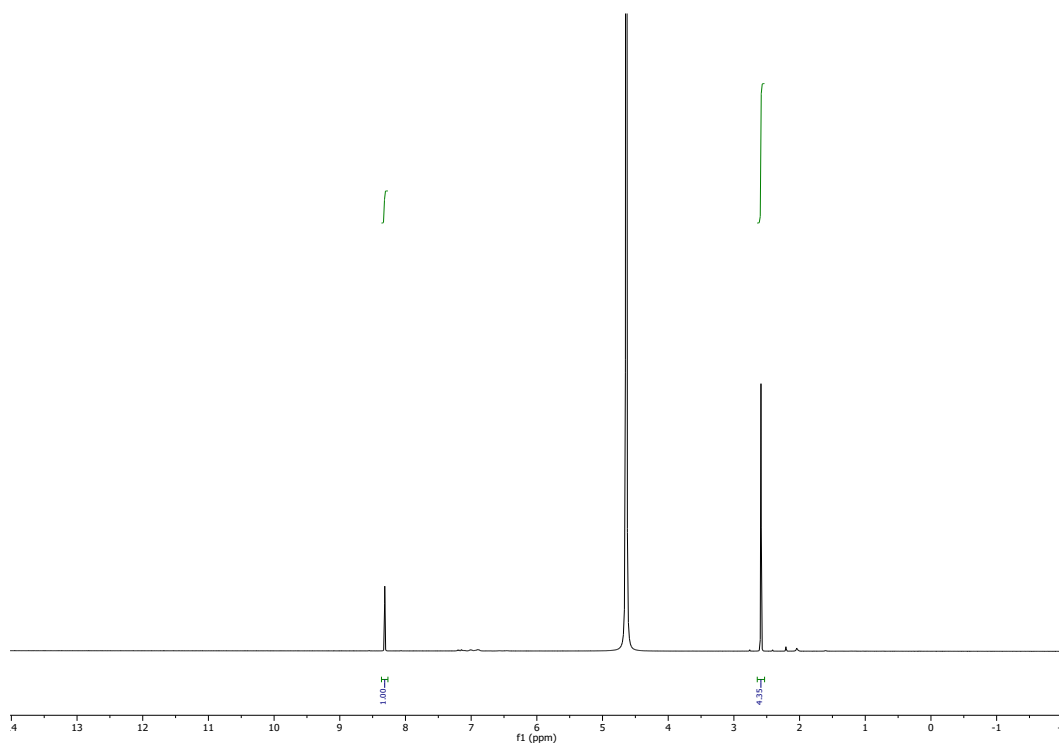


Figure S8. NMR data belonging to table 2, entry 5.

Table S2. ¹H NMR peak data belonging to table 2 (main text) and Figures S3 and S6-8.

Entry	Ratio of DMSO to formate integral
1	106.08
2	50.21
3	3.58
4	4.35
5	4.05

¹H NMR Data belonging to table 3 (main text)

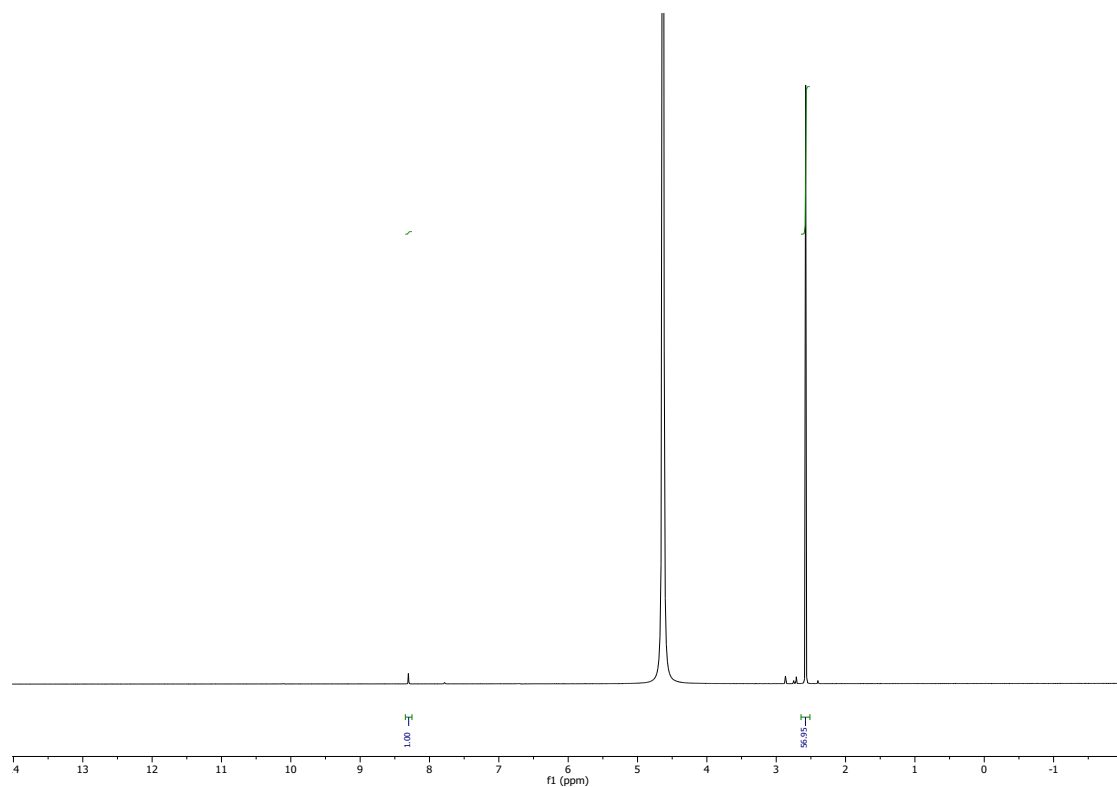


Figure S9. NMR data belonging to table 3, entry 1.

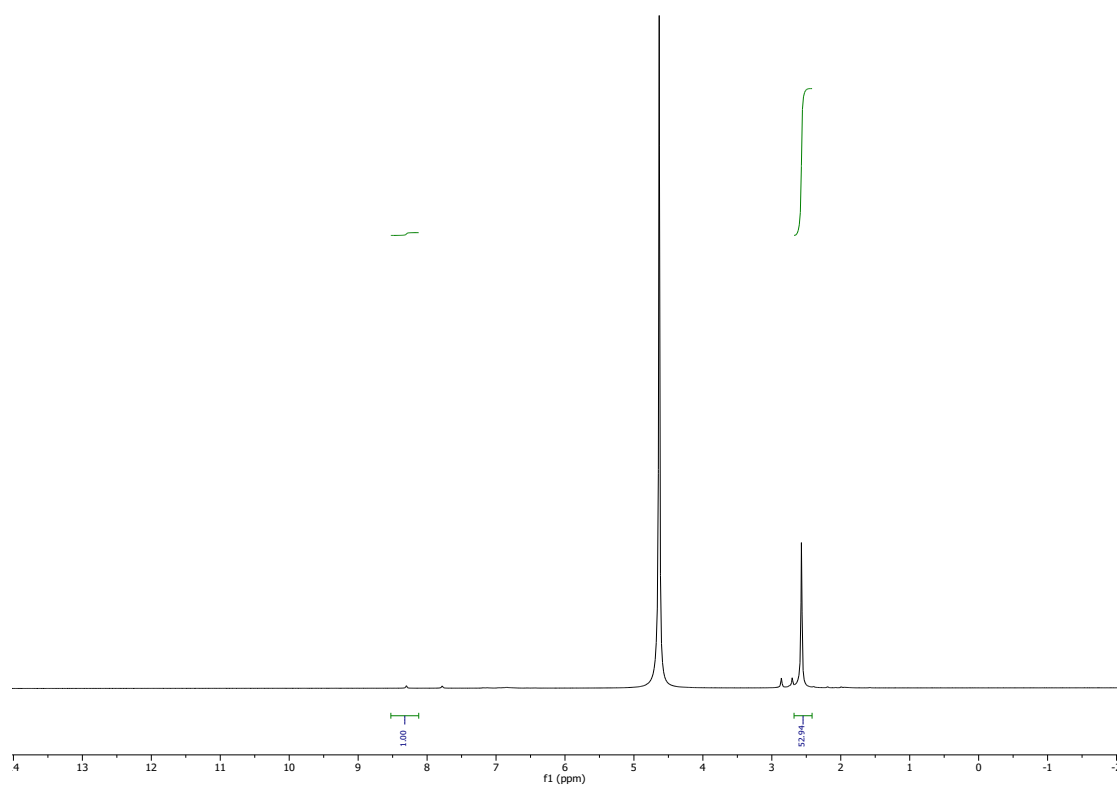


Figure S10. NMR data belonging to table 3, entry 2.

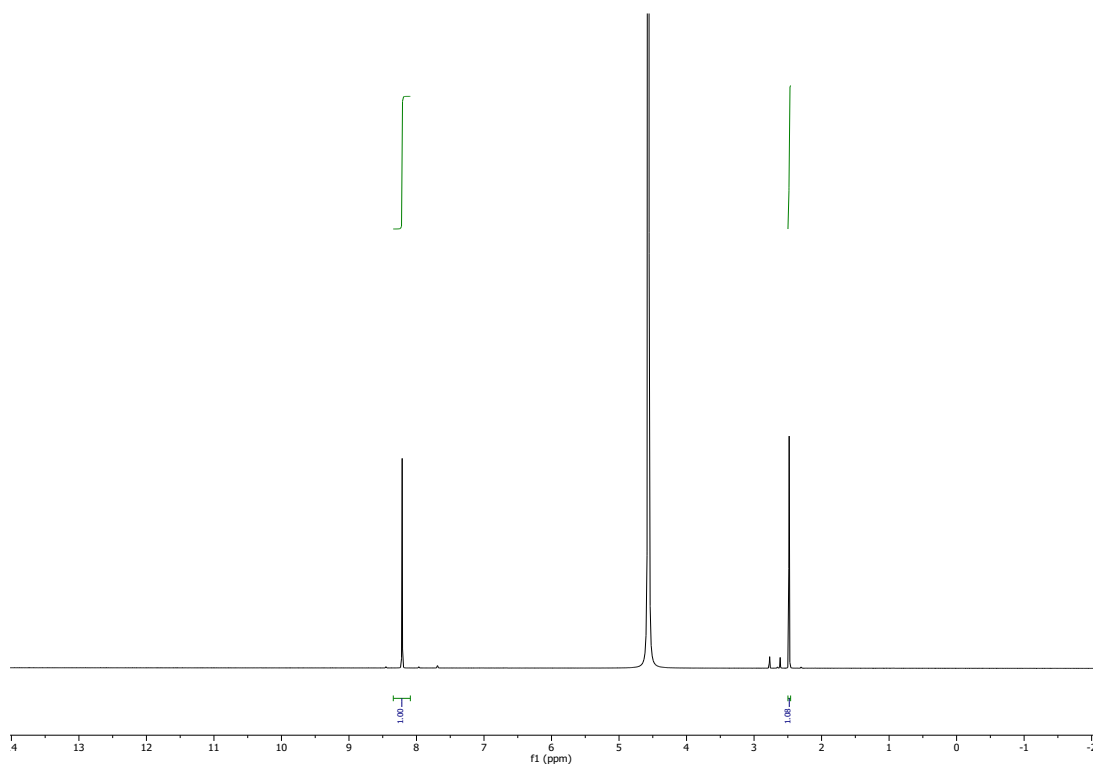


Figure S11. NMR data belonging to table 3, entry 3.

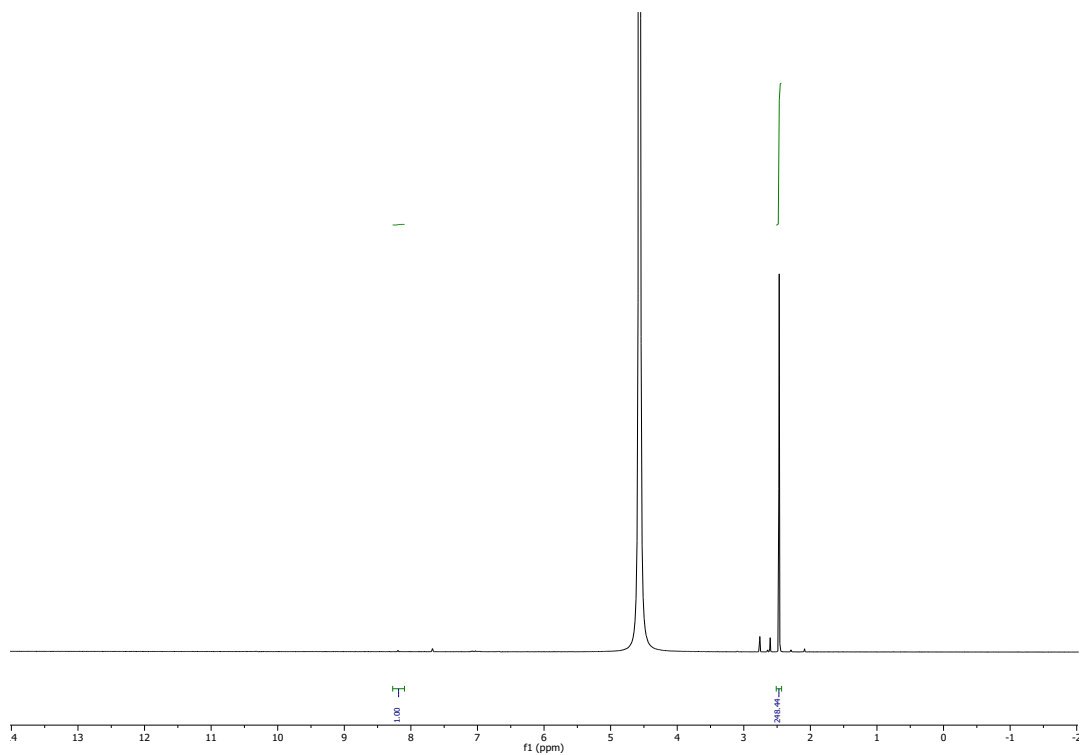


Figure S12. NMR data belonging to table 3, entry 4.

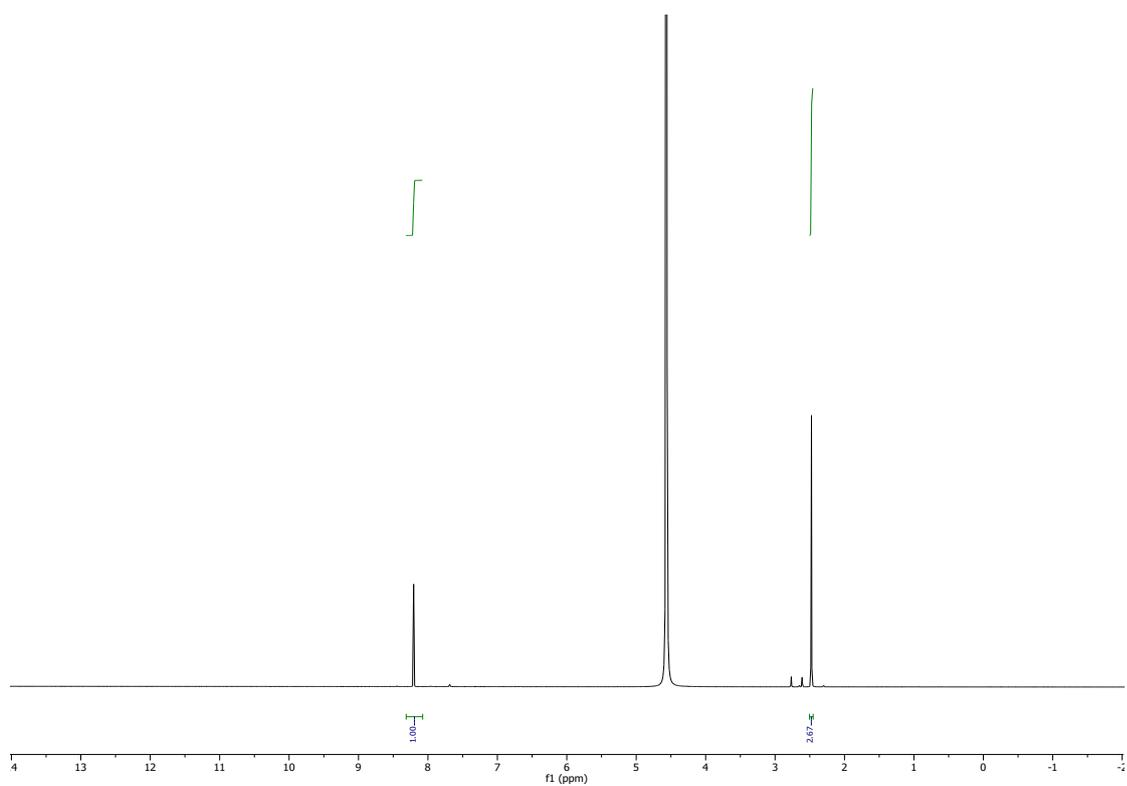


Figure S13. NMR data belonging to table 3, entry 5.

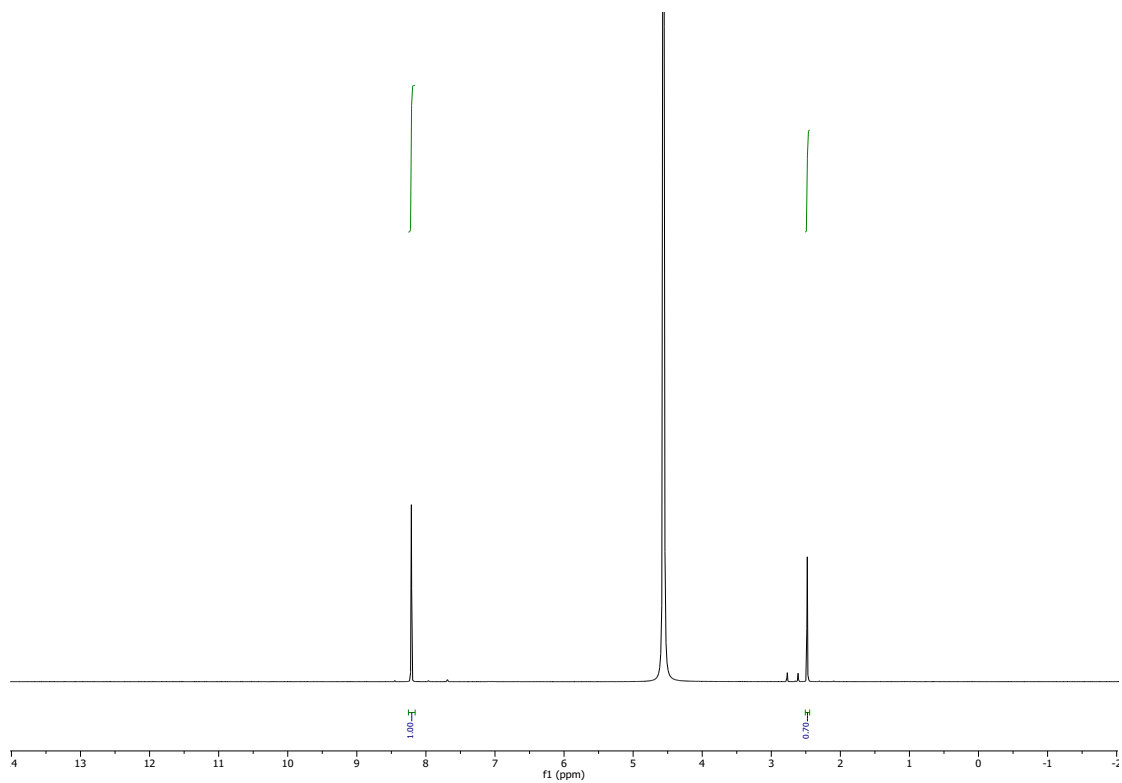


Figure S14. NMR data belonging to table 3, entry 6.

Table S3. ¹H NMR peak data belonging to table 3 (main text) and Figures S9-S14.

Entry	Ratio of DMSO to formate integral
1	56.95
2	52.94
3	1.08
4	248.44
5	2.67
6	0.70

Table S4. Data accompanying Figure 2 (main text), with KHCO_3 as the substrate, for the 2.5 mmol data point (the other values are found in Table 3, main text and Table S3).

Entry	KHCO_3 (mmol)	Ratio of DMSO to formate integral	Yield (%)	TON
1	2.5	2.80	60.3	25648

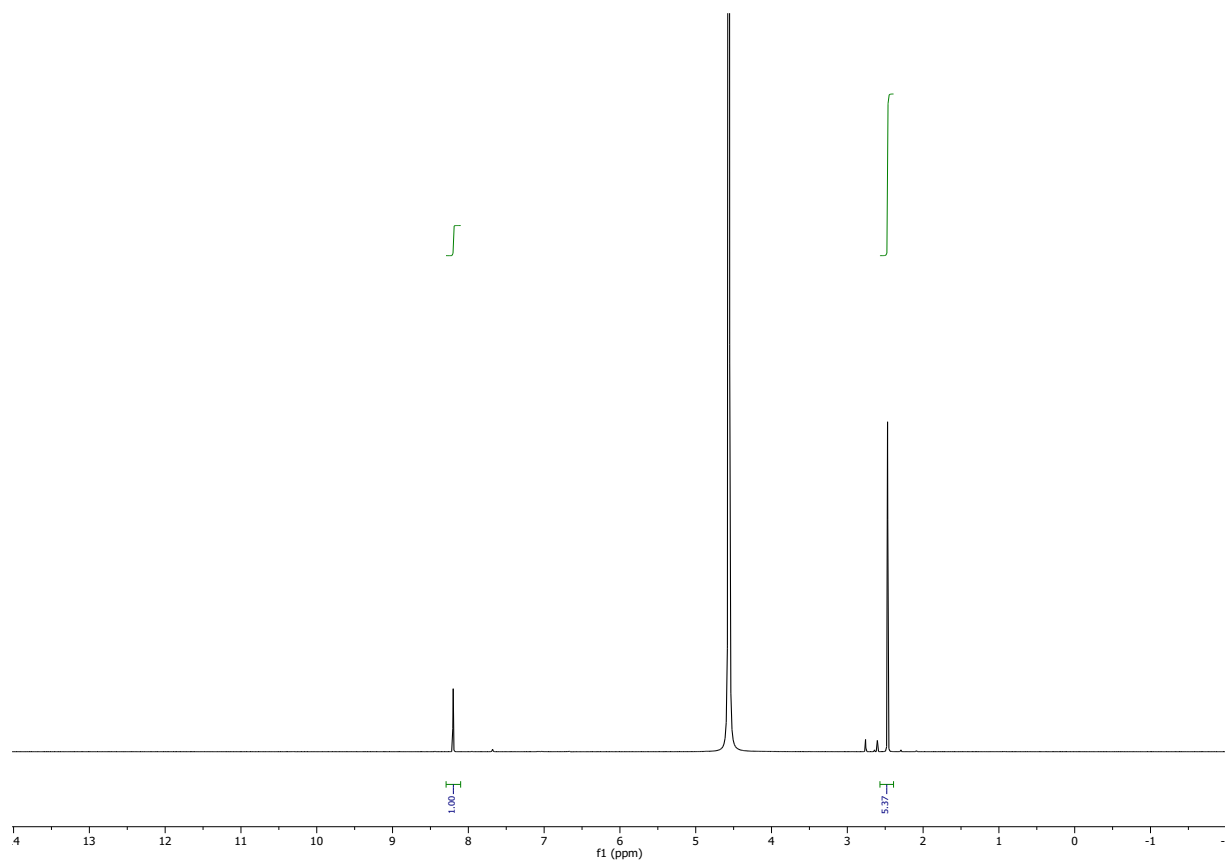


Figure S15. NMR data belonging to table S4, entry 1.

Table S5. Data accompanying Figure 2 (main text), with NaHCO_3 as a substrate.

Entry	NaHCO_3 (mmol)	Ratio of DMSO to formate integral	Yield (%)	TON
1	5	2.80	60.3	25648
2	7.5	2.26	49.8	31777
3	10	2.58	32.7	27835

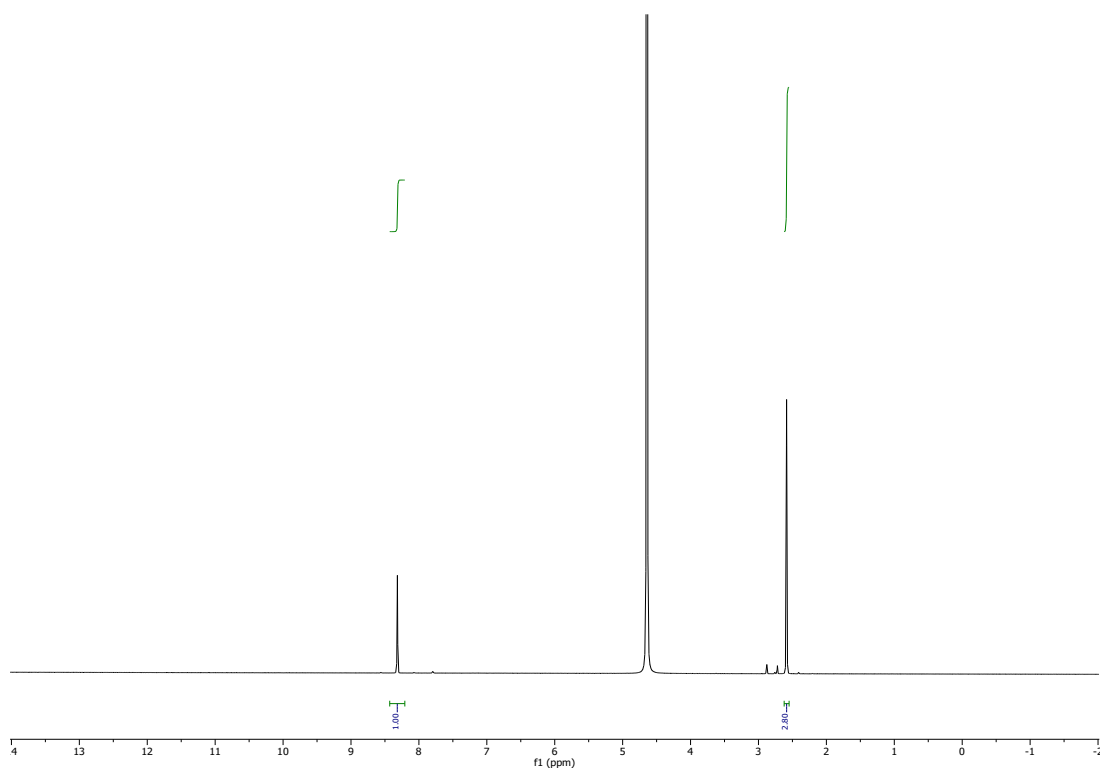


Figure S16. NMR data belonging to table S5, entry 1.

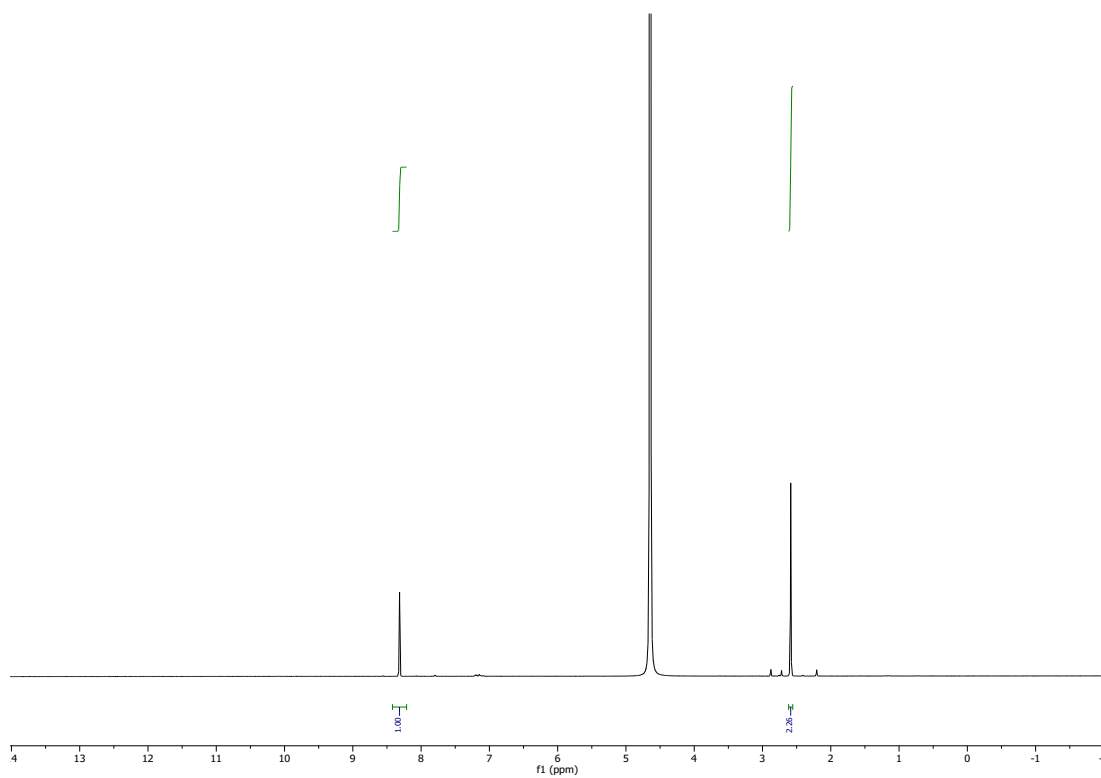


Figure S17. NMR data belonging to table S5, entry 2.

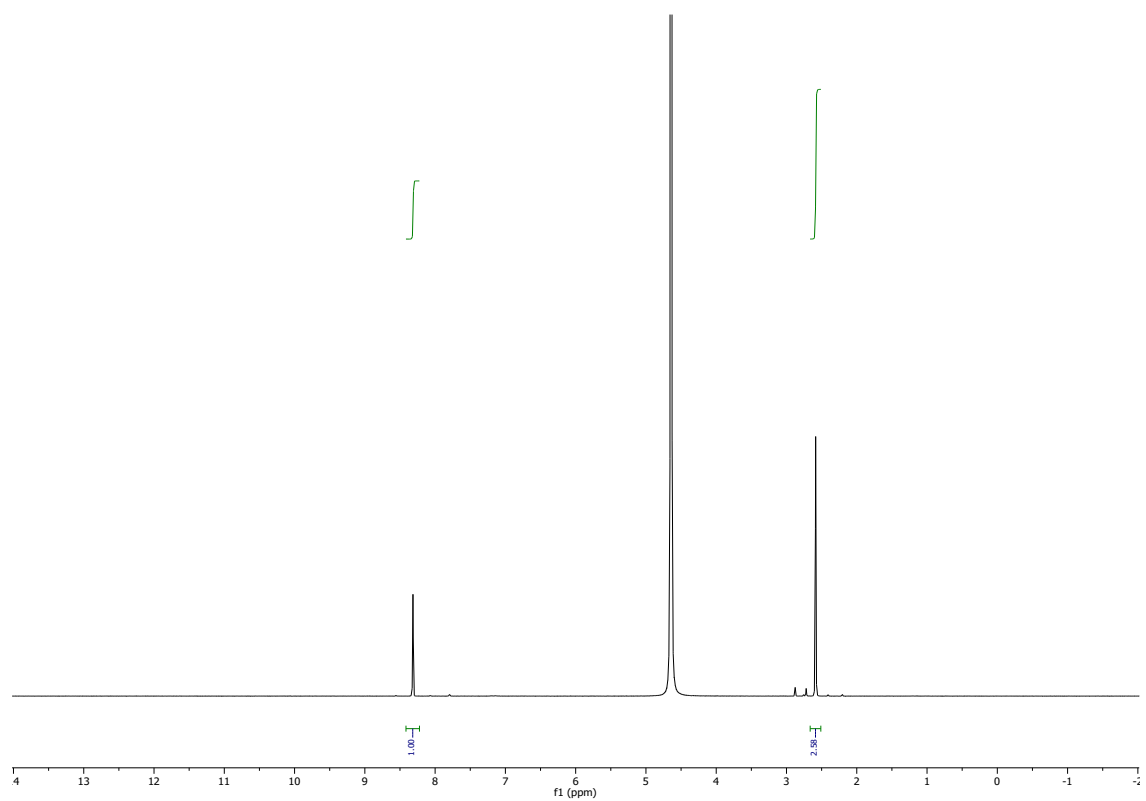


Figure S18. NMR data belonging to table S5, entry 3.

Table S6. Data accompanying Figure 3 (main text), for T = 65 °.

Entry	Pressure (bar)	Ratio of DMSO to formate integral	Yield (%)	TON
1	5	5.02	33.7	14306
2	10	3.37	50.2	21310
3	20	2.70	62.6	26598
4	40	2.31	73.2	31089
5	60	2.29	73.9	31360

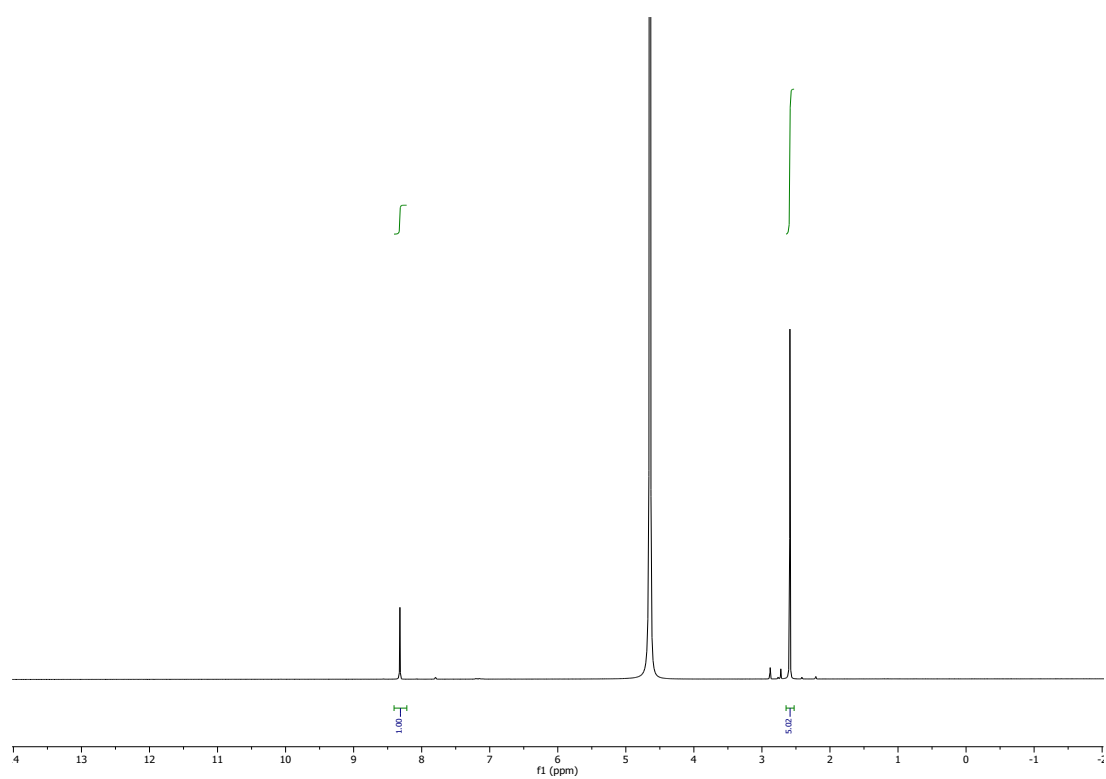


Figure S19. NMR data belonging to table S6, entry 1.

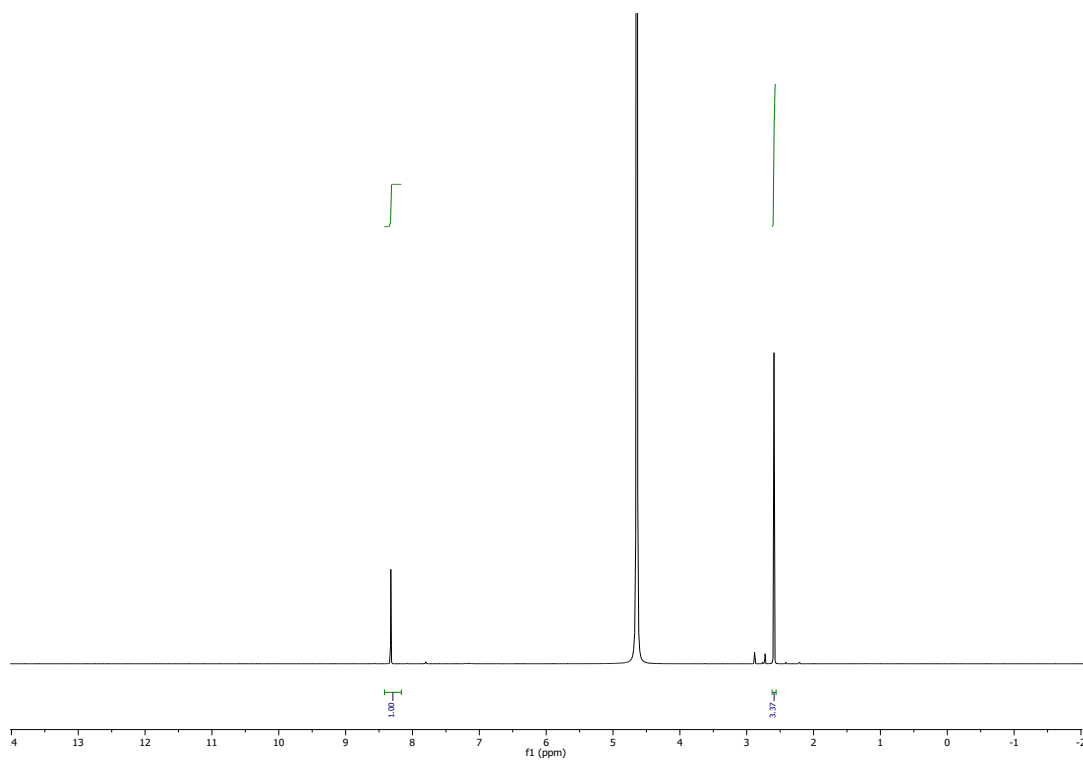


Figure S20. NMR data belonging to table S6, entry 2.

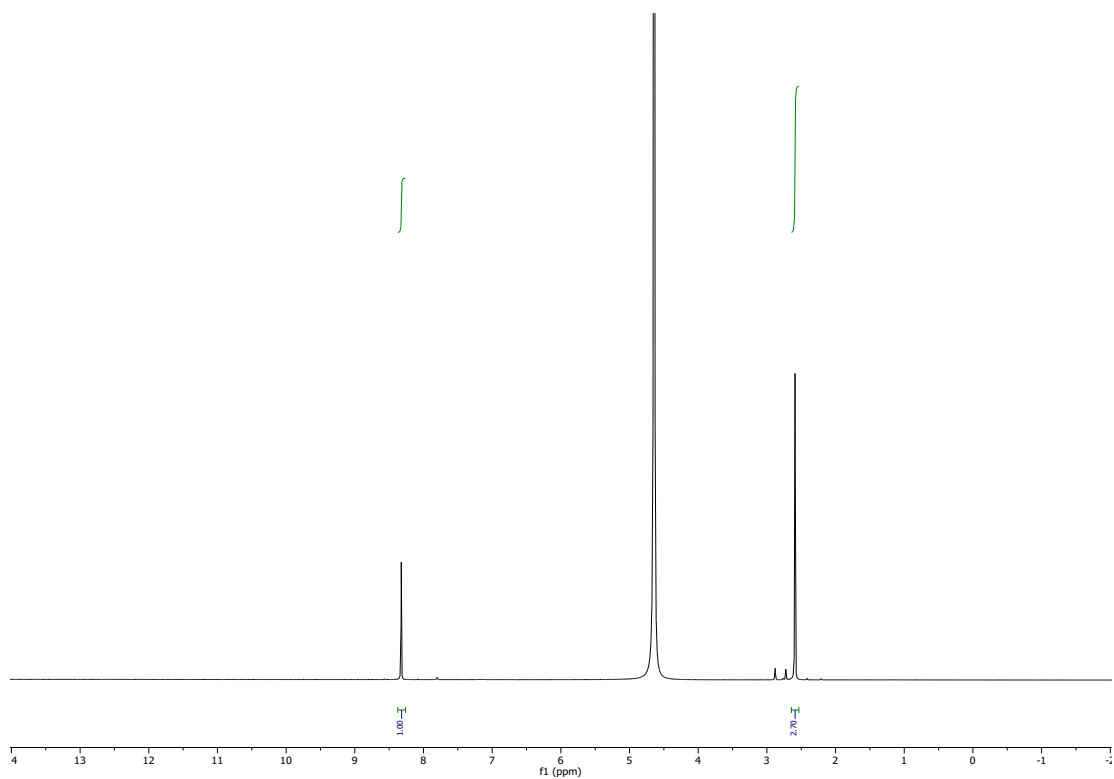


Figure S21. NMR data belonging to table S6, entry 3.

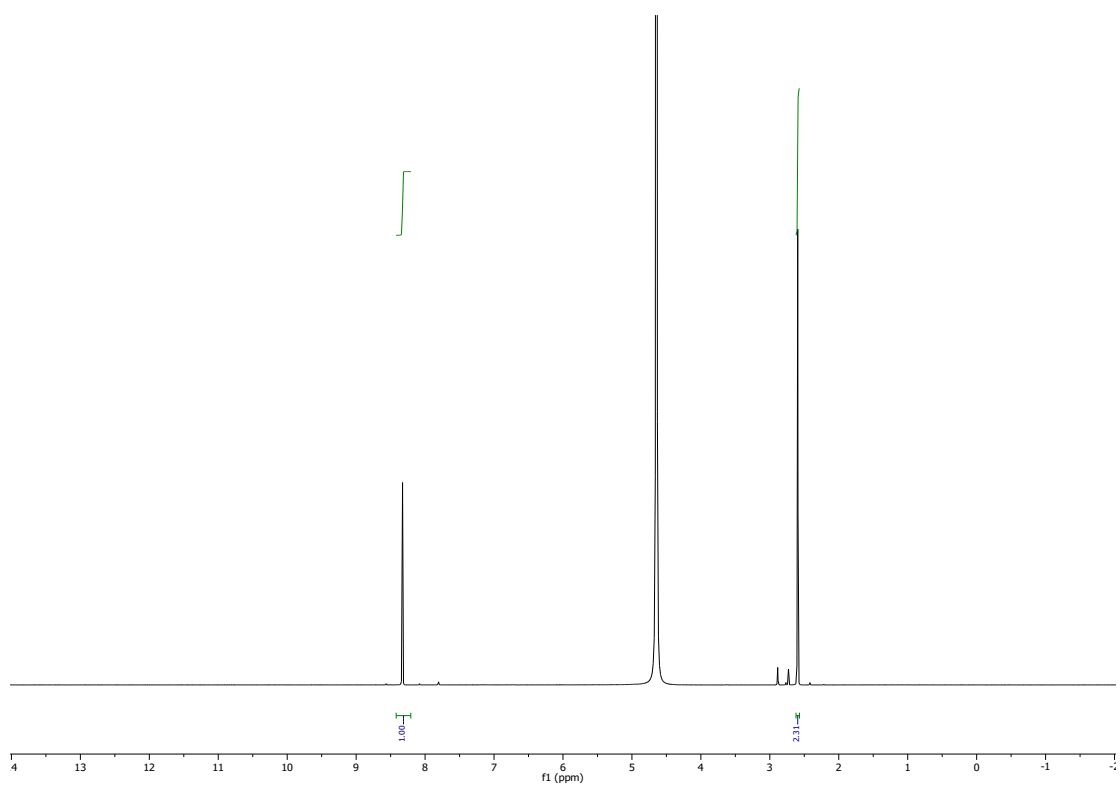


Figure S22. NMR data belonging to table S6, entry 4.

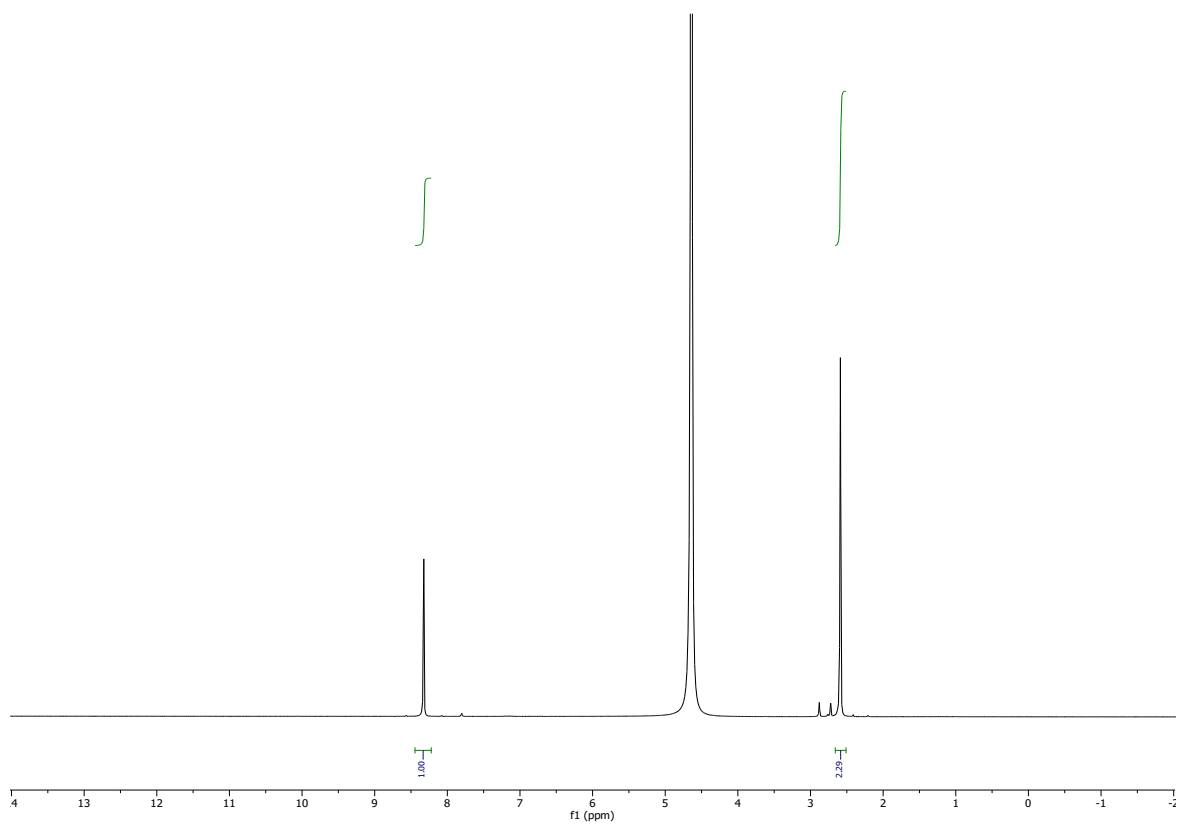


Figure S23. NMR data belonging to table S6, entry 5.

Table S7. Data accompanying Figure 3 (main text), for T = 90 °.

Entry	Pressure (bar)	Ratio of DMSO to formate integral	Yield (%)	TON
1	5	4.86	35.3	14777
2	10	4.80	35.5	14961
3	20	2.84	60.1	25287
4	40	2.32	73.4	30955
5	50	1.89	89.1	37997

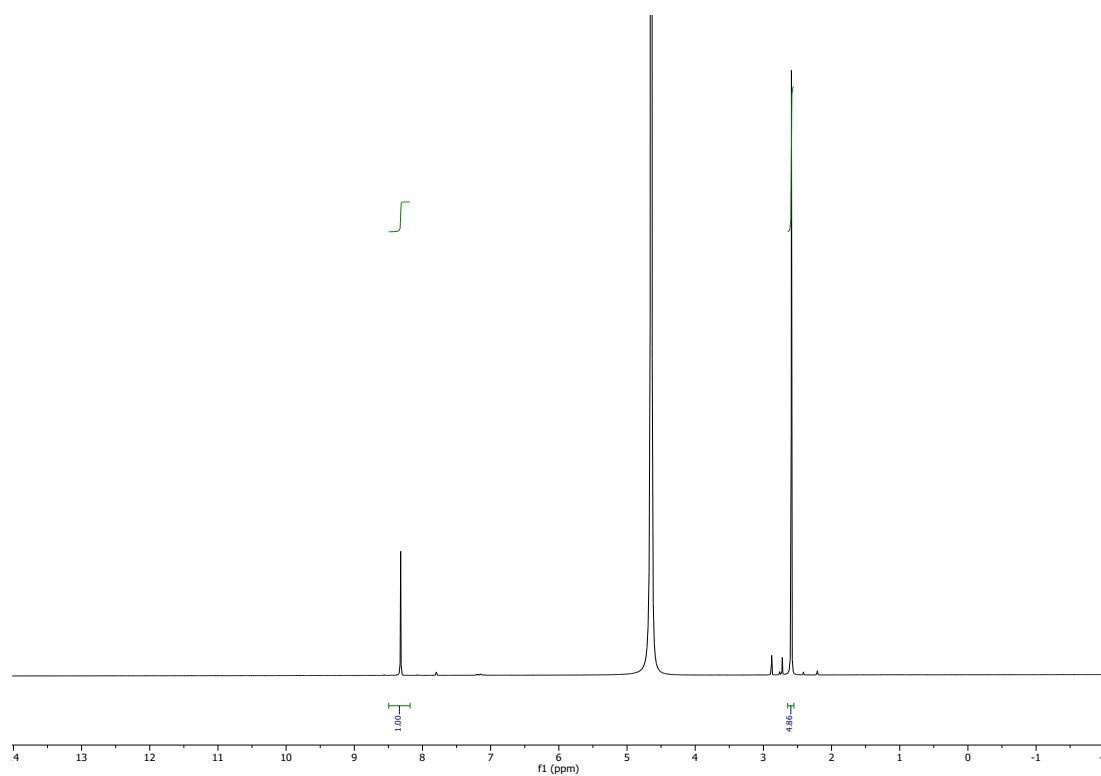


Figure S24. NMR data belonging to table S7, entry 1.

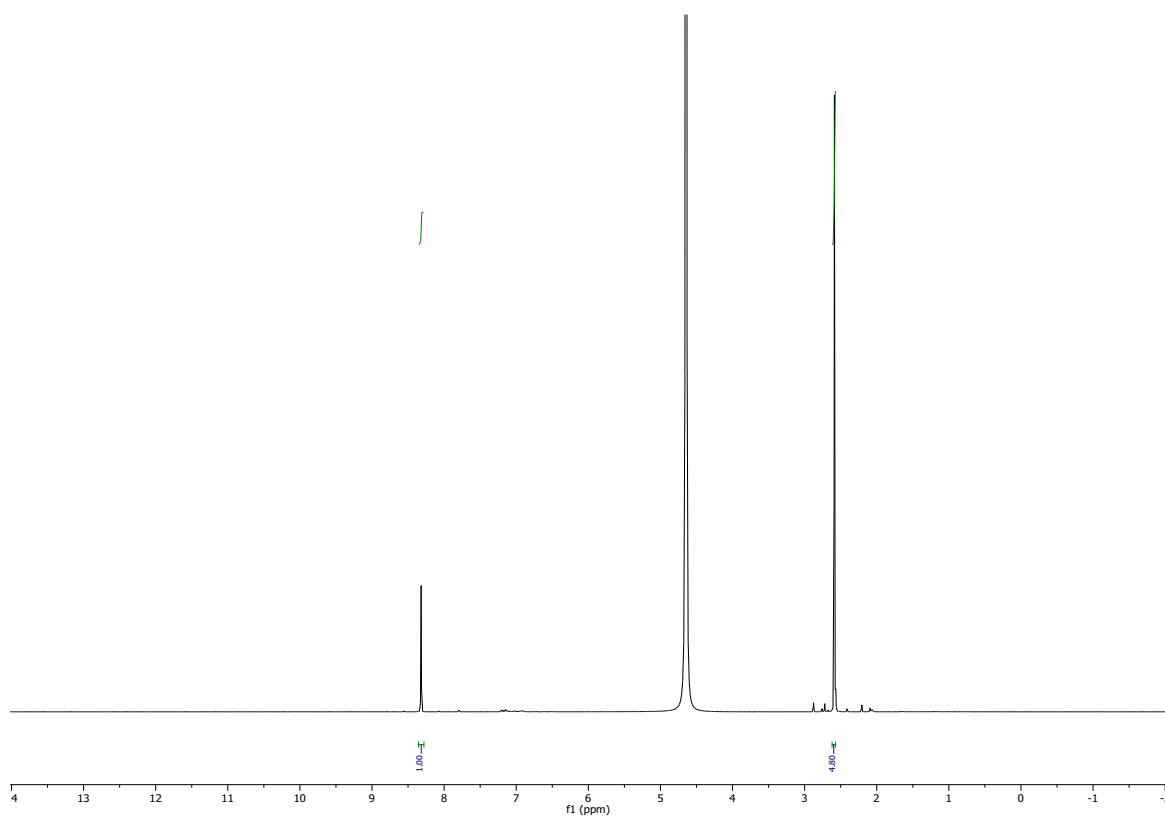


Figure S25. NMR data belonging to table S7, entry 2.

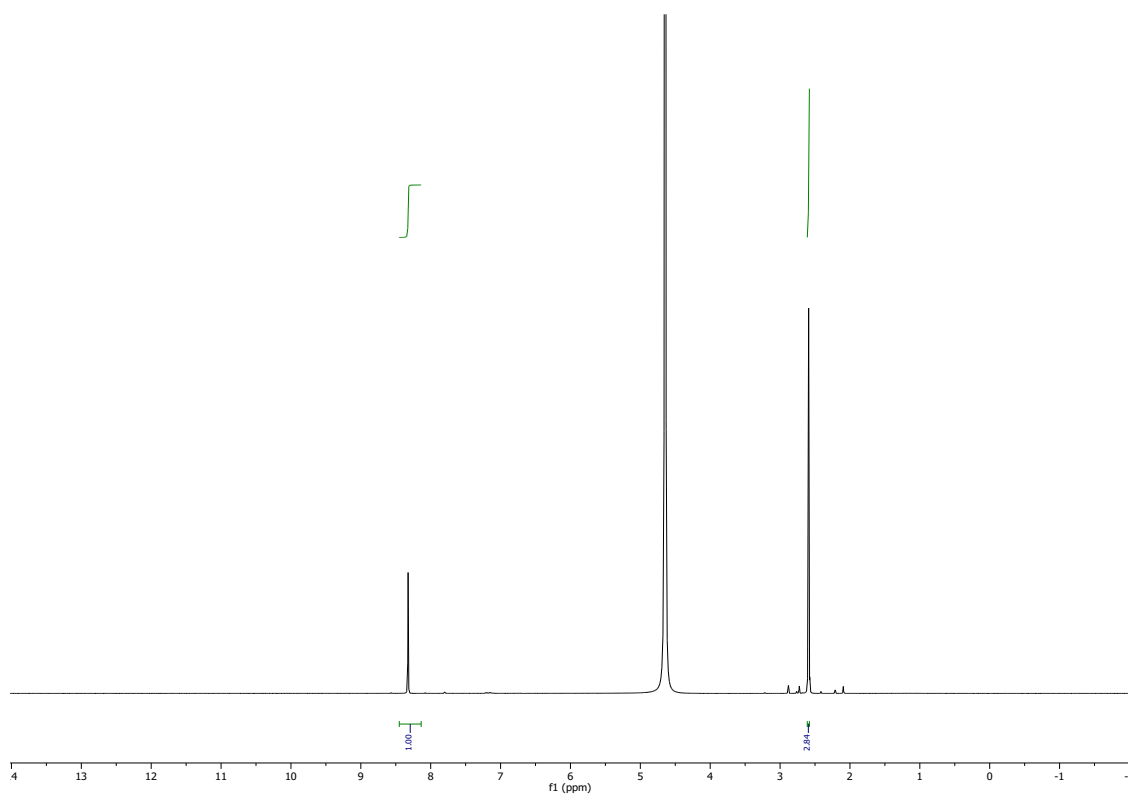


Figure S26. NMR data belonging to table S7, entry 3.

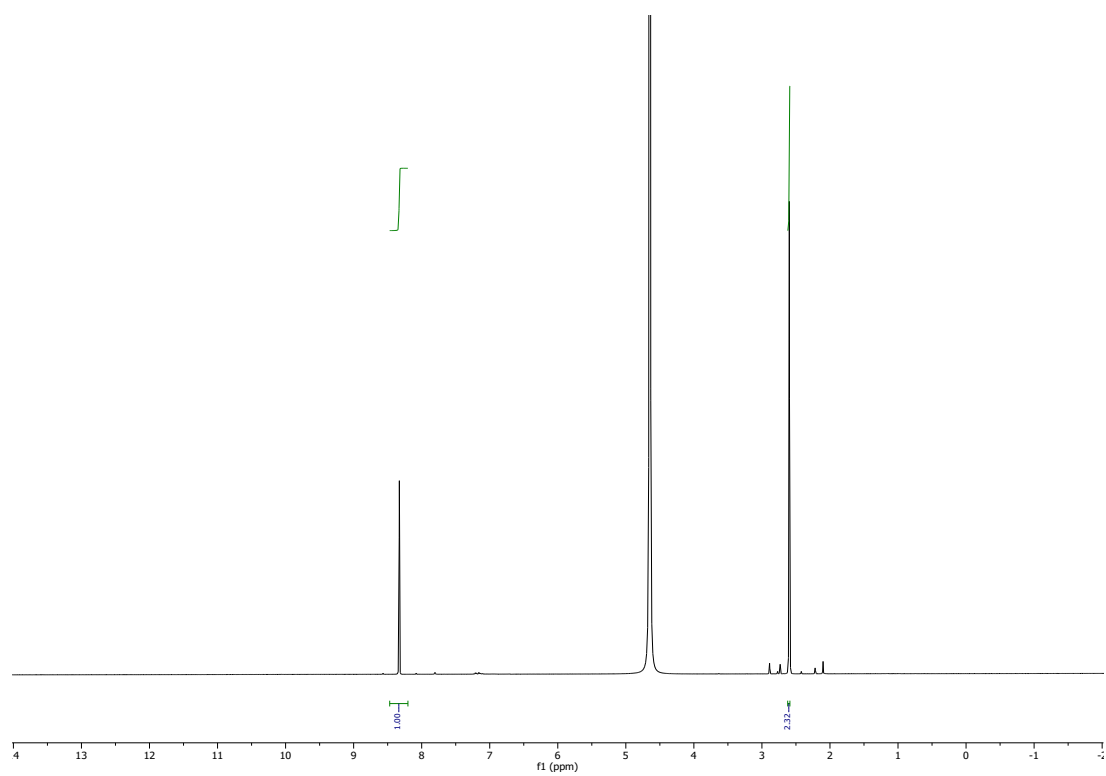


Figure S27. NMR data belonging to table S7, entry 4.

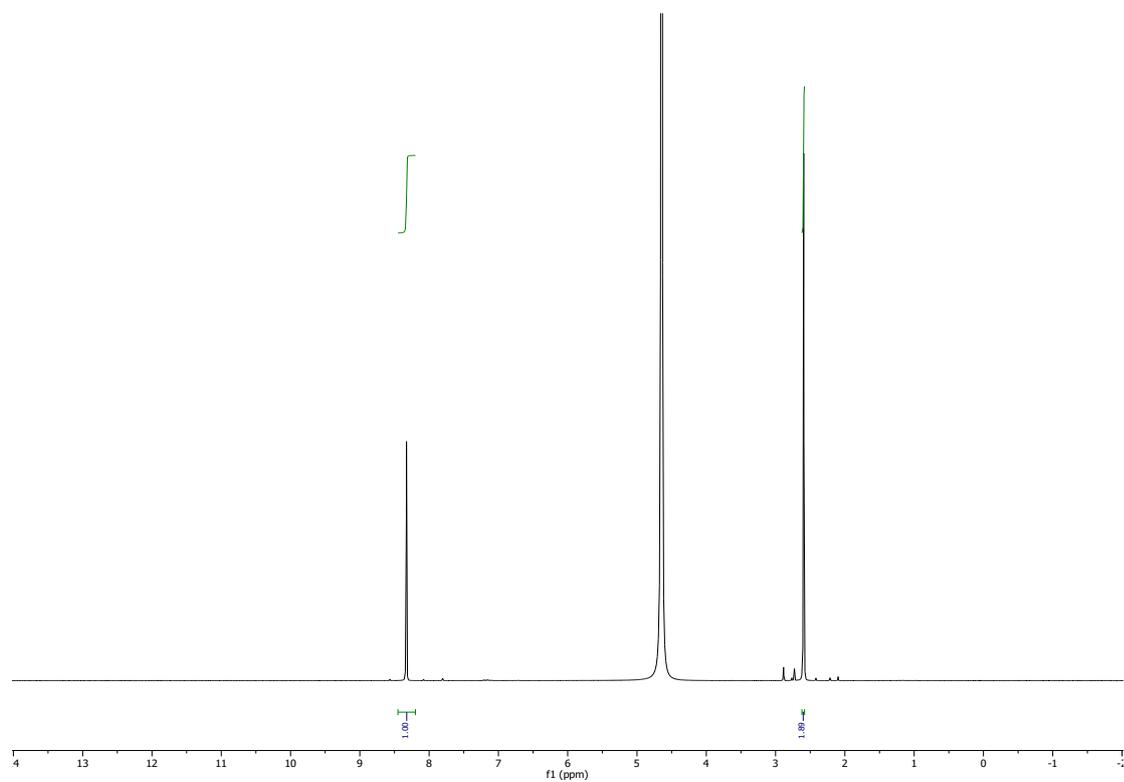


Figure S28. NMR data belonging to table S7, entry 5.

Table S8. Data accompanying Figure 3 (main text), for T = 120 °.

Entry	Pressure (bar)	Ratio of DMSO to formate integral	Yield (%)	TON
1	5	199.01	0.8	361
2	10	9.00	18.8	7979
3	20	5.00	33.8	14363
4	40	2.54	66.6	28274
5	53	2.06	82.1	34862

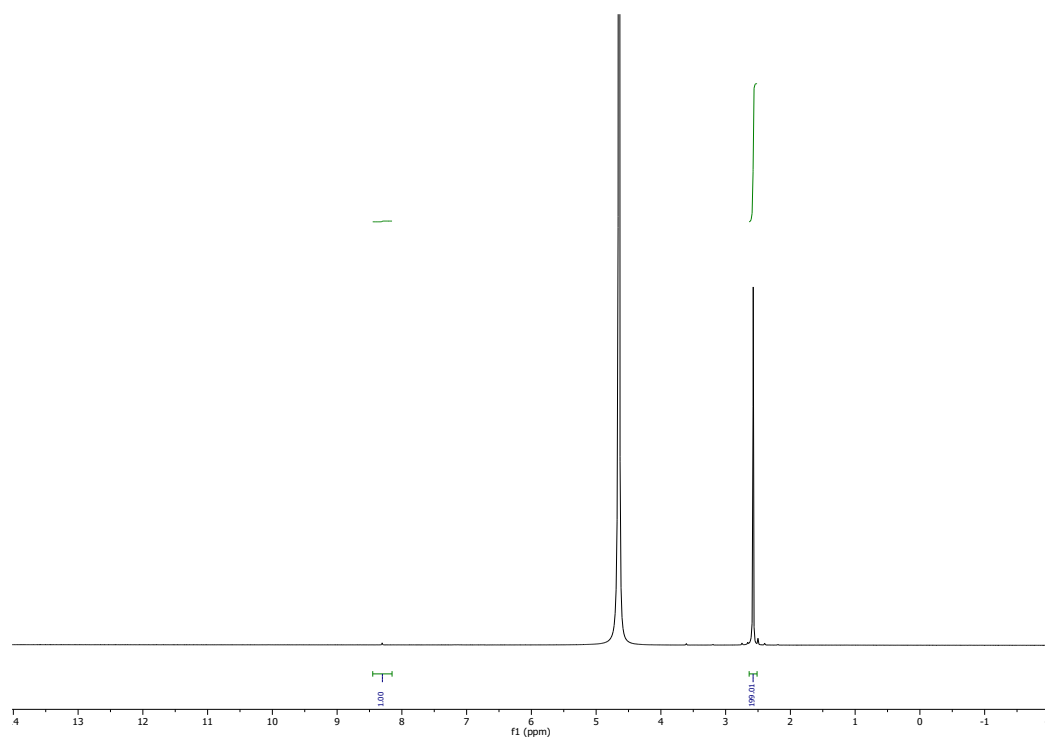


Figure S29. NMR data belonging to table S8, entry 1.

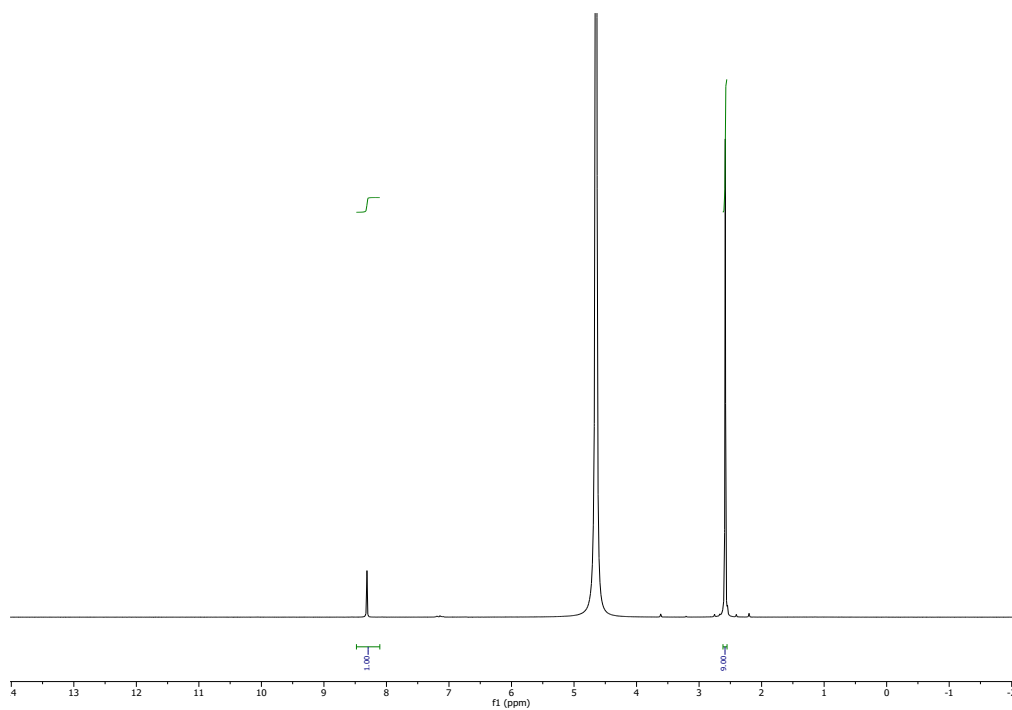


Figure S30. NMR data belonging to table S8, entry 2.

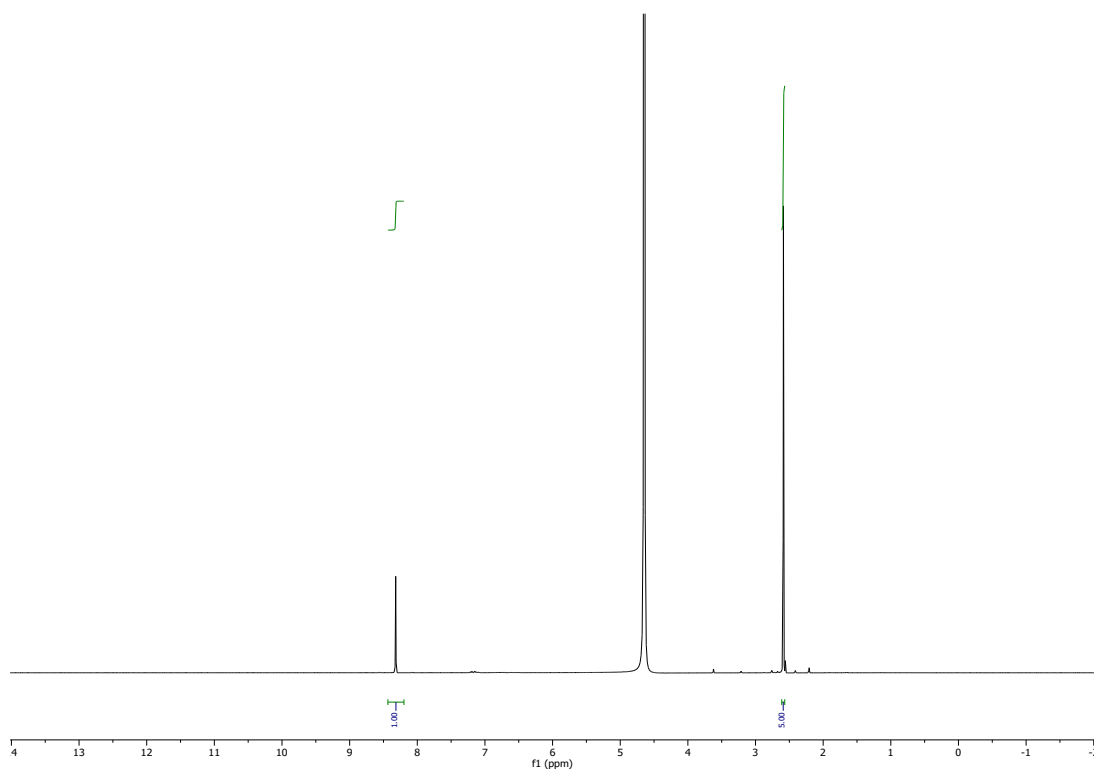


Figure S31. NMR data belonging to table S8, entry 3.

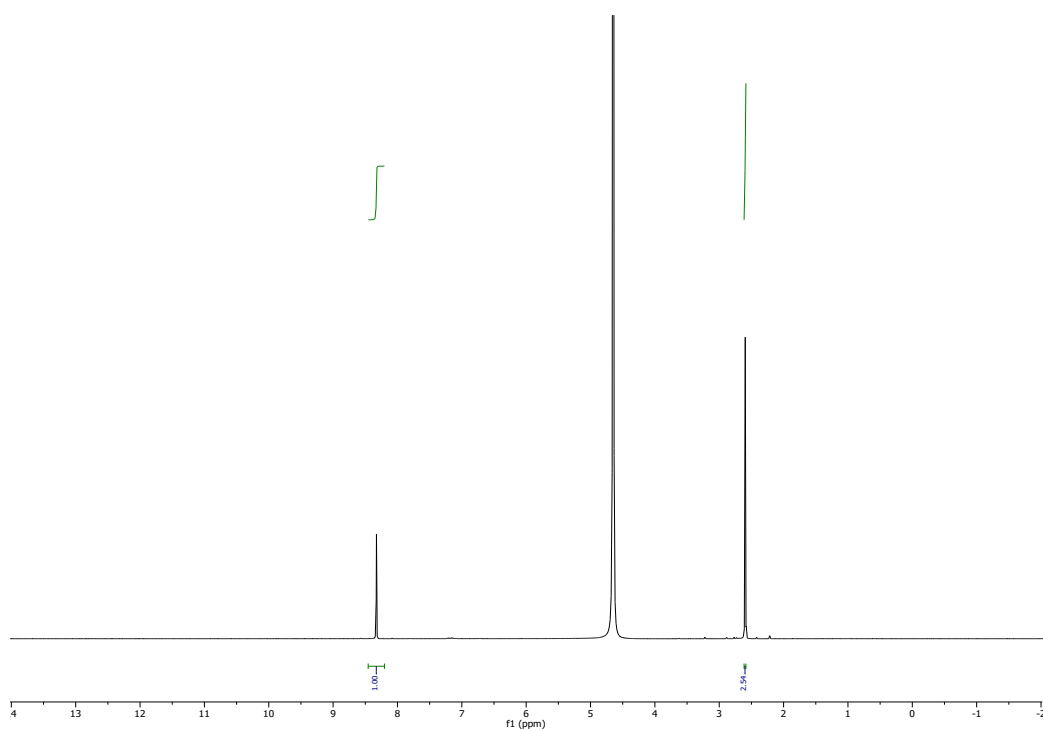


Figure S32. NMR data belonging to table S8, entry 4.

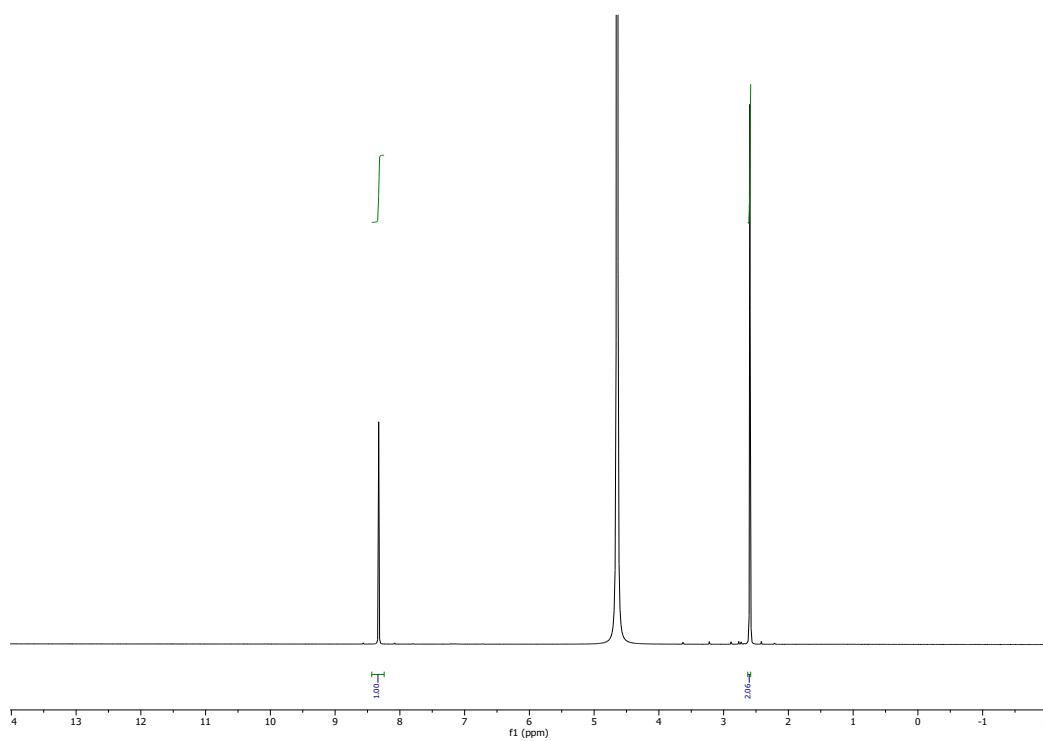


Figure S33. NMR data belonging to table S8, entry 5.

¹H NMR data accompanying data provided in Table 4

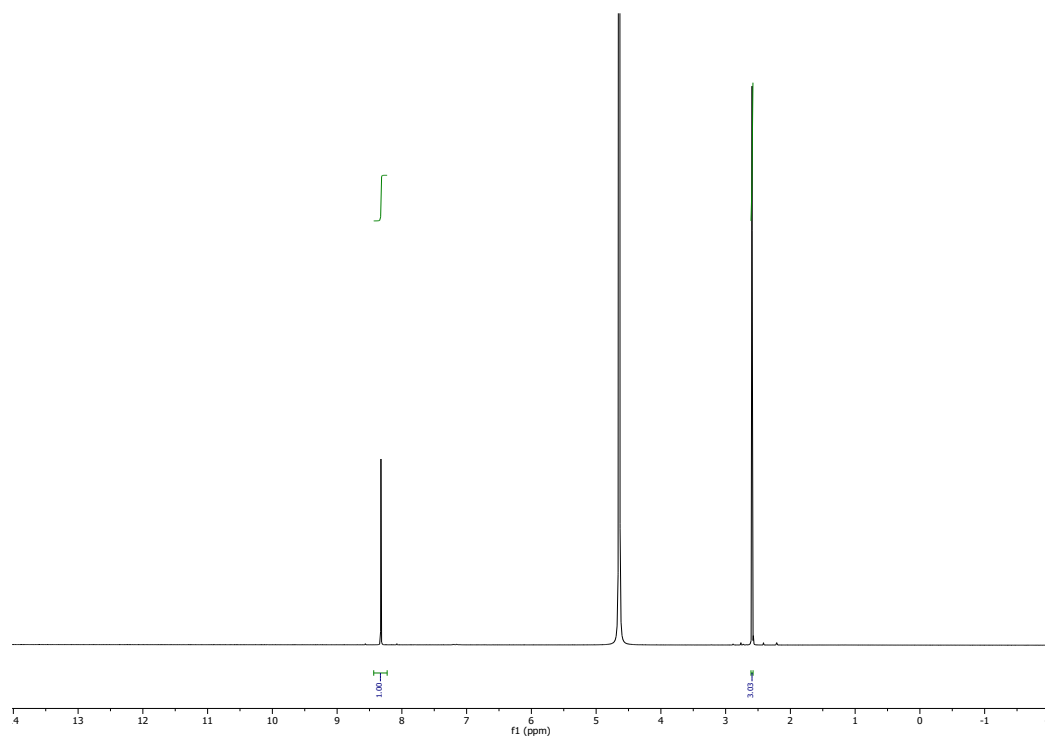


Figure S34. NMR data belonging to table S9, entry 1.

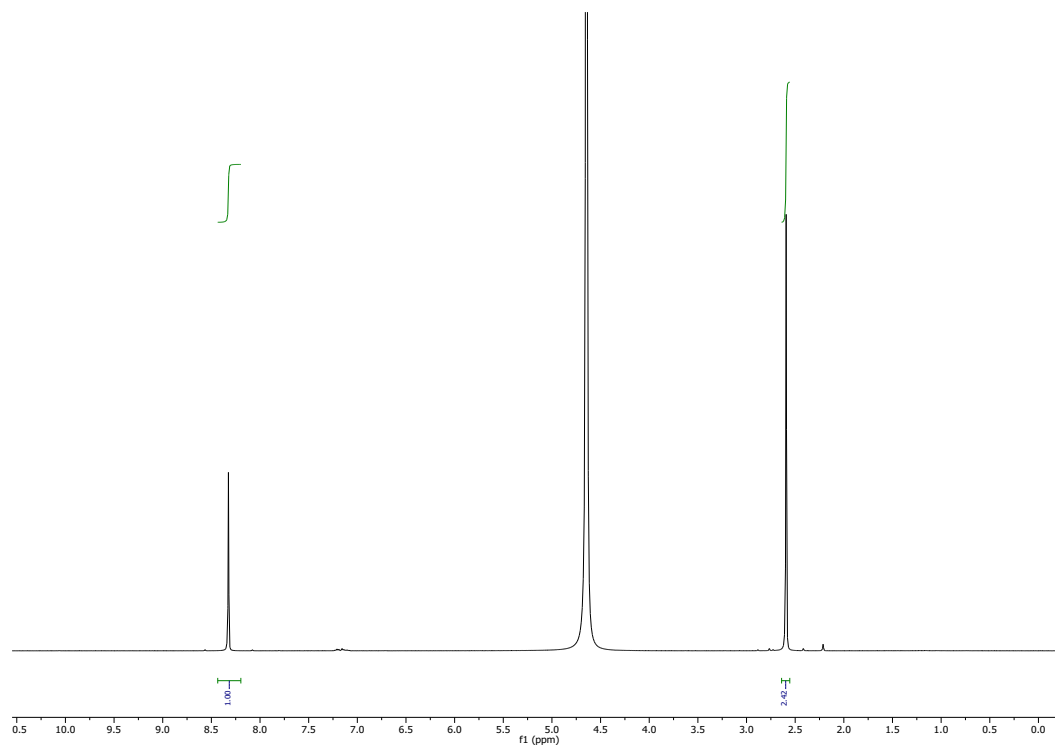


Figure S35. NMR data belonging to table S9, entry 2.

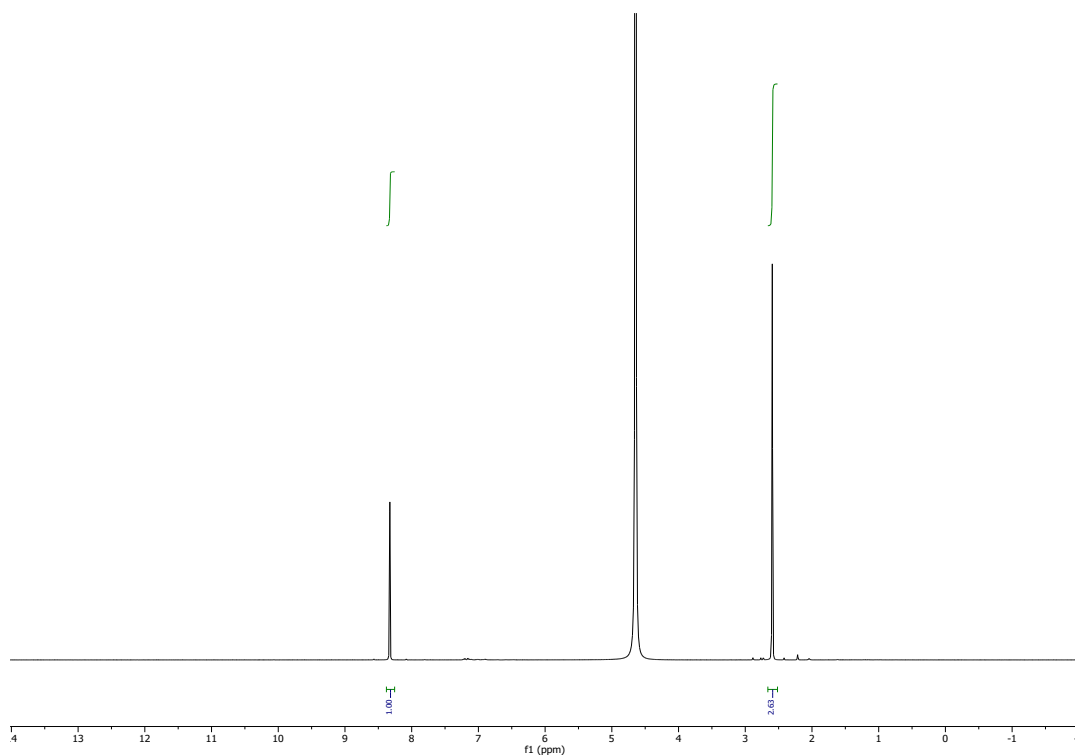


Figure S36. NMR data belonging to table S9, entry 3.

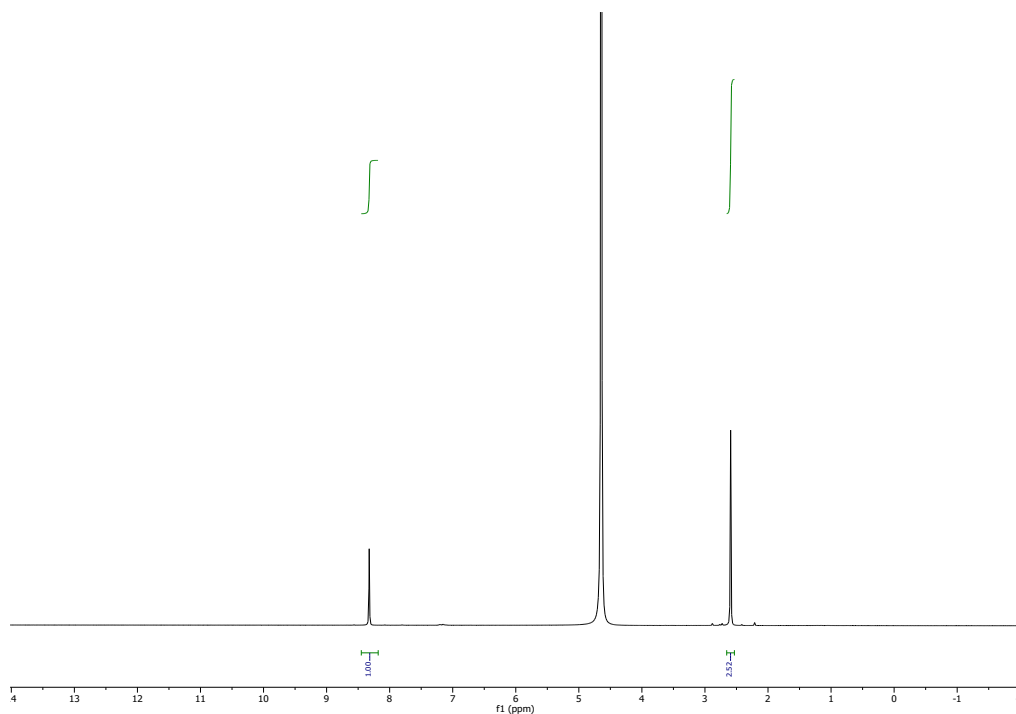


Figure S37. NMR data belonging to table S9, entry 4.

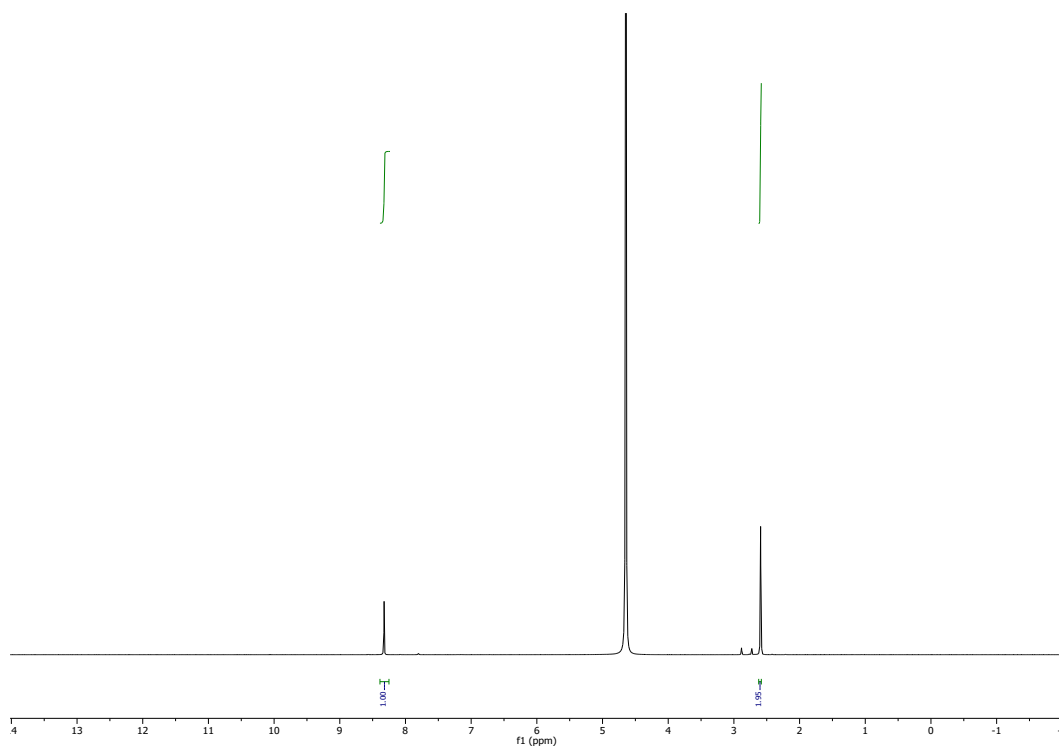


Figure S38. NMR data belonging to table S9, entry 5.

Table S9. ¹H NMR peak data belonging to table 4 (main text) and Figures S34-S38.

Entry	Ratio of DMSO to formate integral
1	3.03
2	2.42
3	2.63
4	2.52
5	1.95

References:

- i. Gnanaprakasam, B.; Zhang, J.; Milstein, D. *Angew. Chem. Int. Ed.*, **2010**, *49*, 1468.